FORCES IN THE FLOW OF LIQUID HE II

G. VAN DER HEIJDEN

FORCES IN THE FLOW OF LIQUID HE II

PROEFSCHRIFT

TER VERKRIJGING VAN DE GRAAD VAN DOCTOR IN DE WISKUNDE EN NATUURWETENSCHAPPEN AAN DE RIJKSUNIVERSITEIT TE LEIDEN, OP GEZAG VAN DE RECTOR MAGNIFICUS DR. W. R. O. GOSLINGS, HOOGLERAAR IN DE FACULTEIT DER GENEESKUNDE, VOLGENS BESLUIT VAN HET COLLEGE VAN DEKANEN TE VERDEDIGEN OP WOENSDAG 10 MEI 1972, TE KLOKKE 14.15 UUR

DOOR

GERRIT VAN DER HEIJDEN
GEBOREN TE BOSKOOP IN 1939

1972
DRUKKERIJ J. H. PASMANS, 'S-GRAVENHAGE

PROMOTORES:

DR. H.C. KRAMERS

PROF.DR. K.W. TACONIS

STELLINGEN

1. Het is aanbevelenswaardig het onderzoek van de diverse typen stromingen van vloeibaar helium, zoals beschreven in dit proefschrift, voort te zetten met een methode om de drukverschillen meer direkt te meten en tevens het temperatuurgebied en het snelheidsgebied uit te breiden.

2. De door Kidder en Blackstead gemeten drukverschillen in bijna isotherme stromingen van vloeibaar helium bij 1,09 K, zijn waarschijnlijk voor een belangrijk gedeelte veroorzaakt door een stroming van het normale fluïdum en niet door de superfluïde stroming alleen zoals deze auteurs onderstellen.
J.N. Kidder en H.A. Blackstead, Proc. of the 9th int. Conf. on low Temp. Phys. LT9, 1964, p.331.
Hoofdstuk III van dit proefschrift.

3. De calibratie van de snelheid van het superfluïde helium in het experiment van Rosenshein, Taube en Titus is aan bedenkingen onderhevig.
J.S. Rosenshein, J. Taube en J.A. Titus, Phys. Rev. Lett. 26(1971)298.

4. De door Brewer en Edwards gebruikte formule voor het verband tussen de warmtestroomdichtheid in, en het temperatuurverschil over een capillair met vloeibaar helium, is in de gebruikte benadering niet volledig.
D.F. Brewer en D.O. Edwards, Proc. Roy. Soc. A251(1959)247.
Hoofdstuk I van dit proefschrift.

5. De beweringen van Kokkedee, dat bij een symmetrisch supergeleidend dubbelpuntkontakt de kritische stroom nul wordt indien uitwendig een magneetveld wordt aangelegd dat overeenkomt met een oneven aantal halve fluxquanta in het omsloten oppervlak, en dat de kritische stroom als funktie van het aangelegde veld oscilleert met een periode die overeenkomt met twee fluxquanta, zijn beide onjuist.
J.J.J. Kokkedee, Ned. Tijdschrift voor Natk. 37(1971)485.
R. de Bruyn Ouboter en A.Th.A.M. de Waele, Progress in low Temp. Physics VI, hoofdstuk 6, red. C.J. Gorter, uitg. North-Holland Publ.Comp.; Physica 42(1969)626.

6. Het verdient aanbeveling het vaste punt van de IPTS-68 (International Practical Temperature Scale of 1968) bij 27,102 K te definieren met behulp van het kookpunt van de isotoop ^{20}Ne in plaats van met het kookpunt van natuurlijk neon.

7. Om het direkte spin-roosterrelaxatieproces in geconcentreerde zouten te onderzoeken, verdient het de voorkeur metingen te verrichten aan poederpreparaten die niet zijn verkregen door fijnwrijven van grotere kristallen.

8. Het onderscheid dat in de wet op het voortgezet onderwijs wordt gemaakt tussen akten van bekwaamheid tweede en derde graad is meer het gevolg van een historisch gegroeide situatie, dan van onderwijskundig denken.
Art. 34 van de wet op het voortgezet onderwijs.

9. Het verdient aanbeveling de veiligheidsvoorschriften voor laagspanningsinstallaties zodanig te wijzigen, dat in nieuwe woningen alleen maar stopkontakten voorzien van een aardkontakt mogen worden aangelegd.

10. Voor het slagen van een interdisciplinair samenwerkingsverband in de sociale en medische gezondheidszorg, is het noodzakelijk dat men in de desbetreffende opleidingen reeds in een vroeg stadium hierop wordt voorbereid.

11. Het door Paulus gebruikte voorbeeld van het enten van een wilde loot op een tamme olijfboom, is in strijd met de door boomkwekers gebruikte veredelingsmethode.
De brief van de apostel Paulus aan de Romeinen, hoofdstuk 11.

Stellingen behorende bij het proefschrift van G. van der Heijden.
(10-5-1972)

Ann Annette

CONTENTS

Introduction

According to the theories of Tisza [1], Landau [2], and London [3], liquid ^{4}He below T = 2.18 K, the "lambda temperature", may be considered to consist of two components: a non-viscous superfluid component with density ρ_s, and a normal viscous component with density ρ_n. The velocities of the two components, v_s and v_n, may have different values. The properties of the flowing liquid at not too small velocities appeared to be more complicated than a simple two-fluid theory could explain. In order to describe these "supercritical" effects, Gorter and Mellink [4] introduced a mutual friction force F_{sn} between the two fluids. Eventually this mutual friction was explained by means of an interaction of vortices, moving with the superfluid, and the thermal excitations of the normal fluid (Hall and Vinen [5]). The possible existence of quantized vortices was put forward by Onsager [6] and Feynman [7]. The supercritical effects are in many ways comparable with turbulence in ordinary liquids. In particular the experiments of Staas, Taconis and Van Alphen [8], could be explained by means of a turbulence of the whole liquid, completely analogous to turbulence in an ordinary liquid.

The experiments described in this thesis deal with types of stationary flow in which the two fluids can be forced to flow simultaneously, with independently adjustable velocities, through a capillary. From the observed temperature differences, and the differences of level heights in manometers, the frictional forces acting on and between the two fluids, could be obtained as functions of the velocities (v_s, v_n). Only relatively small values of the velocities v_s and v_n could be studied: the limits are respectively 10 cm/s and 20 cm/s.

In the present apparatus, that part of the velocity plane (v_s, v_n) where the relative velocity $v_r = v_n - v_s$ is small, could be studied. Therefore the dependence of the mutual friction force on v_r, for small values of v_r, could be obtained. Wiarda and Kramers [9,10], used a similar apparatus for the study of the attenuation of second sound.

The presentation of the results is as follows. In chapter I, experimental details are given, together with results for flow with $v_s \approx 0$. In chapter II, the results for flow with $v_n \approx 0$ are reported. In chapter III, the

results for types of flow with v_n and v_s both unequal to zero are given, together with a general discussion.

The three chapters will be published as separate papers in Physica.

References

1) Tisza, L., Nature 14(1938)913.
2) Landau, L.D., J. Phys. USSR 5(1941)71 and 11(1947)91.
3) London, H., Proc. Roy. Soc. A171(1939)484.
4) Gorter, C.J. and Mellink, J.H., Physica 15(1949)285.
5) Hall, H.E. and Vinen, W.F., Proc. Roy. Soc. A238(1956)215.
6) Onsager, L., Suppl. Nuovo Cimento VI(1949)249.
7) Feynman, R.P., Progress in low Temp. Phys., ed. C.J. Gorter, North-Holland Publ. Comp. (Amsterdam, 1964) vol.I, chap.II.
8) Staas, F.A., Taconis, K.W. and Van Alphen, W.M., Physica 27(1961)893.
9) Wiarda, T.M., Thesis (Leiden, 1967).
10) Kramers, H.C., Superfluid Helium, ed. J.F. Allen, Academic Press (London and New York, 1966) p.199.

CHAPTER I

FLOW WITH SMALL SUPERFLUID VELOCITY

Synopsis

The simultaneous flow of the superfluid and normal component of liquid He II through a capillary is studied. The manner in which the two fluids are forced to flow with independently adjustable velocities is described. The temperature and chemical-potential drop over the capillary are measured, from which the pressure drop can be derived. In subcritical as well as in supercritical flow with small v_s, the pressure drop equals the Poiseuille pressure drop of the normal fluid, indicating that the normal fluid is not turbulent, but flows laminarly. No pressure drop of the superfluid has been present. The results on the pressure drop are contrary to the results of other experiments, in which an additional pressure drop has been observed.

1. Introduction

The interaction between the superfluid and the normal component of liquid helium is not well understood. The way this interaction was previously studied, however, was limited to a few types of flow. Most of the flow experiments with liquid helium II fall under one of the following four types:

1) pure superfluid flow: $\overline{v}_n = 0$ [1-8];
2) pure heat transport flow: $\rho_s \overline{v}_s + \rho_n \overline{v}_n = 0$ [9-21];
3) normal fluid flow in a superfluid which is not restricted [22];
4) gravitational flow without a superleak [23,24].

The mean velocities and the densities of the superfluid and normal fluid are denoted respectively by $\overline{v}_s$, ρ_s, $\overline{v}_n$, and ρ_n. The sum of ρ_s and ρ_n equals the total density ρ.

In order to be able to study the hydrodynamics with other velocity combinations as well, Wiarda and Kramers [25-27] constructed an

apparatus in which an adjustable normal fluid flow was superimposed on an adjustable mass flow. With this apparatus, these authors studied the extra attenuation of second sound as a function of $\overline{v}_s$ and $\overline{v}_n$. The present measurements were undertaken with an apparatus similar to that of Wiarda. The temperature and chemical-potential differences over a capillary are measured for combinations of superfluid and normal fluid flows that can be chosen arbitrarily. The results of the measurements on ΔT and $\Delta\mu$ and of the values of $\Delta P = \rho S \Delta T + \rho \Delta\mu$ calculated from this, may be a help for a better understanding of the interdependence and the hydrodynamics of the two fluids. Some preliminary results have already been published [26,28].

It should be stressed that the nomenclature in this thesis is such that a flow will be called subcritical if the chemical-potential difference over the capillary, $\rho\Delta\mu$, is identically zero. Supercritical flows, with $\rho\Delta\mu$ not identically zero, will be called turbulent. Results of turbulent flows shall be discussed using the model of vortex lines in the superfluid as Vinen [10] has proposed. The interaction of the vortices with the excitations of the normal fluid will be described with a mutual friction force.

2. Design of the experiments

2-1. *Principle of the apparatus.* In the apparatus helium flowing through a *capillary* has been examined. Various flow combinations $(\overline{v}_s, \overline{v}_n)$ can be produced by superpositions of normal flow and mass flow, either in the same or in opposite directions. Only the mean values $(\overline{v}_s, \overline{v}_n)$ of the velocities of the two components, averaged over the volume of the capillary, can be derived. In order to allow for investigations of types of flow in which the directions of $\overline{v}_n$ and $\overline{v}_s$ have the same or opposite sign, two different arrangements (a) and b)) of the apparatus have been used.

These two arrangements are shown schematically in fig. 1. The closed circuit, partially filled with liquid helium II and partially with helium gas, consists essentially of the following parts: a heat exchanger (in thermal contact with the surrounding bath), a superleak, the capillary, a standpipe, and a gaslink. In the apparatus type a) dissipation of energy

Fig. 1

Schematic drawing of the two versions of the apparatus.
(H)-Heater; (P)-Pressure; (S)-Superleak;
(T)-Thermometer; (h)-Helium level.

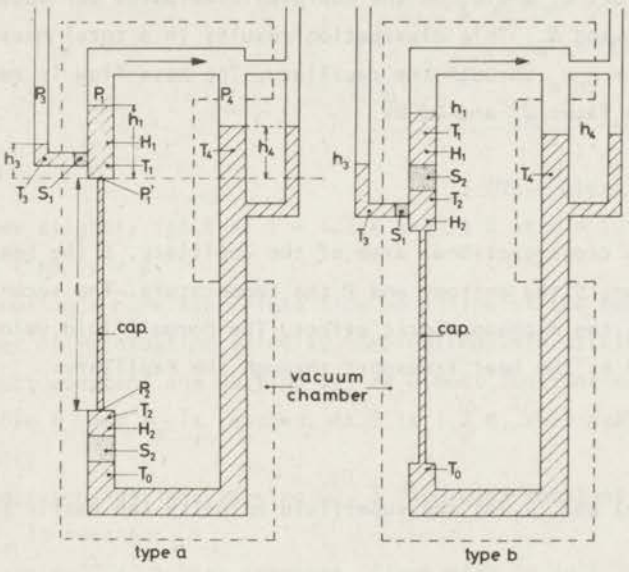

in the heaters H_1 and H_2 results in an evaporation of helium from the standpipe, and a condensation in the heat exchanger. This distillation causes a superfluid flow through the superleak and upward through the capillary. The direction of the gasflow is indicated by an arrow. This direction of flow in the circuit is described with the positive sign. Energy dissipated in heater H_2 is transported upwards through the capillary by a normal fluid flow. This upward flow of normal fluid is accompanied by a descending flow of superfluid. After one of the heaters is switched on, the flow is assumed to be stationary as soon as all the thermometers and helium levels are constant. In this apparatus, flow with adjustable velocity combinations $(\overline{v}_s, \overline{v}_n)$ can be produced. For reasons of simplicity, the mean velocities of the two components, $\overline{v}_s$ and $\overline{v}_n$, will be denoted in the following by v_s and v_n.

The present procedure is contrary to most of the experiments on

superfluid flow in which a level difference is first created. This level difference then causes a superfluid flow, whose velocity can be derived from a measurement of the rate of change of the helium level with time.

2-2. *Calculation of the velocities.*

Type a: Let $\dot{Q}_1$ and $\dot{Q}_2$ be the energies dissipated per second in the heaters H_1 and H_2. This dissipation results in a total mass flow $\rho v = \rho_s v_s + \rho_n v_n$ through the capillary. The mass flow is related to the energy flows $\dot{Q}_1$ and $\dot{Q}_2$ by

$$\dot{Q}_1 + \dot{Q}_2 = A\rho v(L + ST) \ , \tag{2.1a}$$

with A the cross-sectional area of the capillary, L the heat of evaporation, S the entropy and T the temperature. The second term ST represents the mechanocaloric effect. The normal fluid velocity v_n is determined by the heat transport through the capillary:

$$v_n = \frac{\dot{Q}_2}{A\rho ST} \ . \tag{2.2a}$$

From (2.1a) and (2.2a) the superfluid velocity can easily be shown to be:

$$v_s = \frac{\dot{Q}_1 + \dot{Q}_2}{A\rho_s(L + ST)} - \frac{\rho_n}{\rho_s}\frac{\dot{Q}_2}{A\rho ST} \ . \tag{2.3a}$$

Type b: The calculations are slightly different, since $\dot{Q}_2$ does not contribute to the evaporation.

$$v_n = -\frac{\dot{Q}_2}{A\rho ST} \ , \tag{2.2b}$$

$$v_s = \frac{\dot{Q}_1}{A\rho_s(L + ST)} + \frac{\rho_n}{\rho_s}\frac{\dot{Q}_2}{A\rho ST} \ . \tag{2.3b}$$

The velocity regions within reach of the arrangements a) and b) are shown in fig. 2. As may be seen from equations (2.2b) and (2.3b) region b) is limited by the lines $v_n = 0$ and $\rho v = 0$. From (2.2a) and (2.3a) the limits for region a) are: $v_n = 0$ and a line v_s/v_n is constant with a slope

Fig. 2
Velocity values obtainable with the arrangements a) and b).

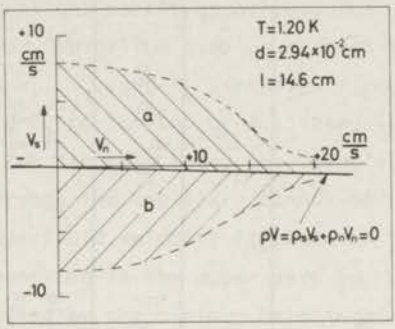

which deviates slightly (10 % at T = 1.2 K and 13 % at T = 1.9 K) from the slope of the line $\rho v = 0$.

By superimposing a pure superfluid flow on a flow of the heat conduction type, a number of interesting velocity combinations are attainable, e.g.:
1) with $\dot{Q}_1$ kept constant and varying $\dot{Q}_2$, an almost constant mass flow, with adjustable v_n and v_s is reached. At T is 1.2 K, this nearly equals v_s is constant;
2) with $\dot{Q}_2$ kept constant and varying $\dot{Q}_1$, a flow with constant v_n and adjustable v_s is reached;
3) with the ratio $(\dot{Q}_1/\dot{Q}_2)$ kept constant, flows with (v_s/v_n) is constant are created. In this way, types of flow such that $v_s = 0$ or $v_s = v_n$ can be produced. From a condition such as $v_s = v_n$, the ratio of the powers that have to be dissipated in the two heaters can be calculated, using the equations (2.2a) and (2.3a):
$(\dot{Q}_1/\dot{Q}_2) = (L/ST)$.
(L/ST) varies from 336 at T = 1.2 K to 16.7 at T = 1.9 K. Thus, by varying both $\dot{Q}_1$ and $\dot{Q}_2$, but keeping their ratio constant at (L/ST) for a given temperature, the two components will move through the capillary on the average with a relative velocity of zero.
In order to obtain pure normal fluid flow ($v_s = 0$) the necessary ratio is

$$\frac{\dot{Q}_1}{\dot{Q}_2} = \frac{\rho_n}{\rho}\left[\frac{L}{ST} + 1\right] - 1.$$

This ratio varies from 8.8 at T is 1.20 K to 6.6 at T is 1.90 K.
The velocities v_n and v_s cannot be chosen arbitrarily large. There are

Table I

Temperature-dependent quantities used in the calculations.

T	ρ	ρ_s	ρ_n	S	L	η_n
K	gcm^{-3}	gcm^{-3}	gcm^{-3}	$Jg^{-1}K^{-1}$	Jg^{-1}	10^{-6} Poise
1.90	0.145543	0.08395	0.06159	0.7310	23.28	13.15
1.70	0.145340	0.11196	0.03338	0.3988	22.95	12.60
1.50	0.145223	0.12879	0.01644	0.1978	22.32	13.55
1.45	0.145216	0.13173	0.01349	0.1628	22.13	14.0
1.35	0.145195	0.13640	0.008795	0.1070	21.71	15.0
1.30	0.145189	0.13822	0.006973	0.0853	21.49	15.6
1.25	0.145185	0.13968	0.005504	0.06723	21.26	16.4
1.20	0.145183	0.14095	0.004235	0.05233	21.03	17.6

Origin of data:

ρ: El Hadi, Z.E.H.A., Durieux, M. and Van Dijk, H., Physica 41(1969)289.

S and η_n: smoothed values from several experiments, calculated by Cornelissen (private communication).

ρ_s and ρ_n: from ρ, S and the second sound velocity measured by Peshkov, V.P., Sov. Phys. JETP 11(1960)580.

L: Van Dijk, H. and Durieux, M., Physica 24(1958)920.

restrictions, caused by the limited dimensions of the apparatus. The chemical-potential difference created by the helium flowing through the capillary, will move the helium levels h_1, h_3, and h_4 (see fig. 1) out of their equilibrium positions. Raising h_1 to the top of its standpipe results in fluid flow through the gaslink. In this case, the velocity of the superfluid component flowing through the capillary cannot be calculated. (The computation of the superfluid velocity is based on the assumption that the helium is transported in the upper part by distillation). Another limit is determined by the minimum heights of h_3 and h_1.

Temperature-dependent quantities used in our calculations are listed in table I.

2-3. *Pressure balance and measuring procedure.* The derivation of the pressure balance as given in the following is only correct if the pressure and temperature differences in the apparatus are small. In that case, a mean value for the entropy S can be used. The critical flow rate for the superleak S_2 is never exceeded. For that reason, the superfluid flow through S_2 is always subcritical, and the chemical-potential drop across S_2 is zero. In the stationary case, with all the helium levels constant, there is not even any liquid flow through S_1, and $\rho\Delta\mu$ across S_1 will also be zero. The pressure balance shall be derived for the apparatus type a), see fig. 1a. P_1, P_3, and P_4 are the pressures of the gas above the liquid.

The pressure at the upper end of the capillary P_1' can be written in two ways:

$$P_1' = P_1 + \rho g h_1 \,, \tag{2.4a}$$

$$P_1' = P_3 + \rho g h_3 + \rho S(T_1 - T_3) \,. \tag{2.5a}$$

The heights h_1, h_3, and h_4 are defined with regard to the upper end of the capillary. $\rho S(T_1 - T_3)$ is the fountain pressure across the superleak S_1. From (2.4a) and (2.5a) the level height h_1 can be computed, since the vapour pressures P_1 and P_3 are known.

The pressure at the lower end of the capillary, P_2, is connected to h_4 by

the relation

$$P_2 = P_4 + \rho g(h_4 + l) + \rho S(T_2 - T_4) \ , \tag{2.6a}$$

with l the length of the capillary.
From the equations (2.4a.....6a) the pressure drop over the capillary $\Delta P' = P_1' - P_2$, can be derived:

$$\Delta P' = \rho g(h_3 - h_4) + \rho S(T_4 - T_3) + (P_3 - P_4) + \rho S(T_1 - T_2) - \rho g l. \tag{2.7a}$$

The last term on the righthand side is the hydrostatic pressure drop between the two ends of the capillary. The extra pressure drop

$$\Delta P = \Delta P' + \rho g l, \tag{2.8}$$

is much more interesting, as it describes the hydrodynamic pressure difference created by the helium flowing in the capillary. Since the temperature difference $(T_4 - T_3)$ is small during all our experiments,

$$P_4 - P_3 = \frac{dP}{dT} (T_4 - T_3) \ . \tag{2.9}$$

The temperature drop over the capillary $(T_1 - T_2)$ is called ΔT. Combining the thermodynamic identity, neglecting velocity contributions,

$$\rho \Delta \mu = \Delta P - \rho S \Delta T \ , \tag{2.10}$$

with the equations (2.7a), (2.8) and (2.9) the chemical-potential drop over the capillary, $\rho\Delta\mu$, is given by

$$\rho \Delta \mu = \rho g(h_3 - h_4) + \left(\rho S - \frac{dP}{dT} \right) (T_4 - T_3) \ . \tag{2.11}$$

Equation (2.11) holds for both arrangements of the apparatus.

The measurements have been performed with one of the thermometers T_1 or T_2 kept constant, within a few micro degrees of the desired temperature, by means of an electronic device. $\dot{Q}_1$ and $\dot{Q}_2$ are fixed at a chosen value by adjusting the voltages V_1 and V_2 across the heaters H_1 (resistance R_1) and H_2 (resistance R_2). Once the thermometers and helium levels are constant, the flow is assumed to be stationary, and the resistances of the thermometers are measured with an A.C. Wheatstone bridge. The helium

levels h_3 and h_4 are determined optically with a cathetometer.

Summarizing:

1) The velocities v_s and v_n are computed from V_1, V_2, R_1, R_2, and the thermodynamic quantities as described in 2-2.
2) The chemical-potential drop over the capillary, $\rho\Delta\mu$, is deduced from h_3, h_4, T_3, and T_4.
3) The temperature drop over the capillary, ΔT, is given by the temperature difference $(T_1 - T_2)$.
4) The hydrodynamic pressure drop ΔP is obtained from the temperature and chemical-potential drop, using the thermodynamic identity (2.10).

2-4. *The experimental set-up.* A more detailed view of the apparatus as used in case a), is shown in fig. 3. The heater H_1 is mounted in a central german silver standpipe A, above the upper end of the capillary. If heat is dissipated in H_1, evaporation of liquid in the standpipe A takes place. The helium gas flows through the film constriction B, and condenses between the brass cylinders C_1 and C_2. The heat flows to the surrounding helium bath, through the walls of cylinder C_2. The superfluid flow circuit is completed by the superleak S_2 and the capillary. Temperatures are measured with the five thermometers T_0,.....T_4, all in the liquid of the apparatus. In order to allow for measurements of the chemical-potential difference over the capillary, both sides of the capillary are connected, via a superleak, to glass standpipes. Stainless-steel capillaries of 2.94×10^{-2}cm and 0.95×10^{-2}cm inner diameter have been used, both 14.6 cm long. The entrances were squarely cut off. The straight capillaries are mounted vertically. In order to avoid too large film flows in the gas part of the circuit, film constrictions are used. The holes are of diameters of 1.5 and 0.5 mm, in combination with the wide and the narrow capillary, respectively.

2-5. *NRS flow.* In the preceding, only situations with the flow circuit partially filled with liquid helium were taken into account. In this way, flow with limited, but adjustable and calculable, v_n and v_s could be

Fig. 3
The apparatus in which flow with v_s and v_n in the same direction can be produced.

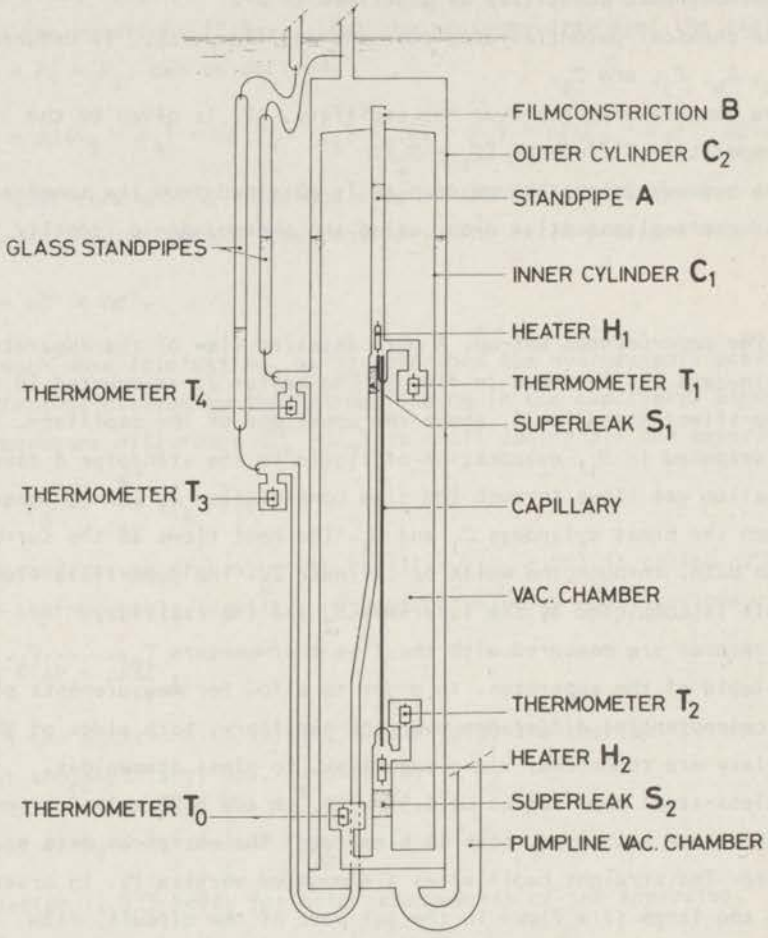

created. With this apparatus, however, another type of flow is also possible. If the apparatus is fully filled with liquid helium and energy is dissipated in heater H_2, there will be a flow of the normal component through the capillary. The velocity of the normal fluid v_n can be computed from equation (2.2a) or (2.2b). The velocity and direction of a possible superfluid flow through the capillary cannot be predicted.

It will be shown that with the apparatus completely filled with liquid helium, the chemical-potential drop over the capillary is zero. Measurements of Van Alphen et al. [29] on the same superleak material (type "A") as is used in the present experiment yielded a critical transfer rate, from which the maximum superfluid velocity in our wide capillary is estimated at 75 m/s. For that reason, a possible flow of superfluid helium through the superleak S_2 is always subcritical. Since there are no chemical-potential drops over other parts of the apparatus, $\rho\Delta\mu$ over the capillary always equals zero.

This type of flow with adjustable normal fluid velocity, possibly accompanied by a superfluid flow whose velocity is not externally restricted, is called NRS flow: Non Restricted Superfluid flow. NRS flow, with $\rho\Delta\mu$ always equal to zero, was studied first by Staas et al. [22]. With NRS flow, the velocities v_n and v_s are not limited by maximum and minimum heights of the helium levels as in the partly filled apparatus. So in spite of the disadvantage that the superfluid velocity v_s cannot be predicted, NRS flow is studied because of the stringent condition $\rho\Delta\mu = 0$ that is imposed on the flow, and because of the high velocities v_n that can be obtained.

3. Corrections.

3-1. *Heat transport through the superleak.* Measurements with the narrow capillary ($d = 0.95 \times 10^{-2}$cm) indicated the importance of a correction for the heat transported through the superleak S_2 (see fig. 3). In order to study this the capillary was removed from the apparatus (type a)), and the holes were closed. With this configuration, the heat transported through the superleak S_2, filled with liquid helium, was measured. At the same time, the film flow was studied (see section 3-2). The superleak S_2 consists of a thin-walled stainless-steel tube, with an I.D. of 5.8 mm, and an O.D. of 6.4 mm filled with jeweller's rouge packed over a length of 10 mm. The powder used is the same material Van Alphen et al. [29] labelled type "A". The particle size of the grains is approximately 7×10^{-5}cm. In the stationary case, the heat current through the superleak $\dot{Q}_{wpl}$ (wall + powder + liquid) equals the power $\dot{Q}_2$ dissipated in the

Fig. 4
The heat conductance of the superleak as a function of temperature.

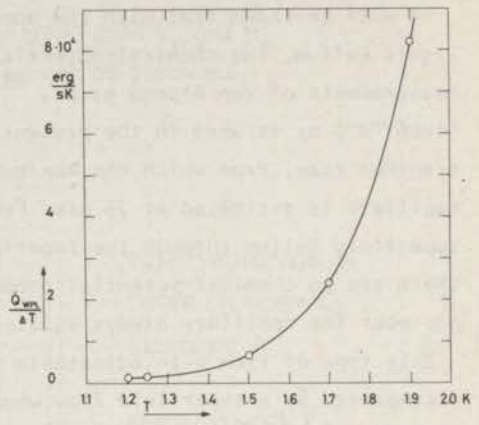

heater H_2. The experimental values of $\dot{Q}_{wpl}$ are listed in table II and plotted in fig. 4. In all the measuring runs with helium flowing through the capillary, a correction to v_n has been applied to account for the heat transport by the superleak S_2.

3-1-1. *Discussion of the heat transport by a superleak.* As shown in fig. 4, $\dot{Q}_{wpl}$, the heat transported by the superleak S_2, strongly depends on temperature. This heat transport is composed of three contributions: from the wall, the jeweller's rouge, and the liquid inside the superleak. The contribution of the wall may be calculated using

$$\dot{Q}_w = \frac{K_{ss} A_w}{l} \Delta T \,, \qquad (3.1)$$

with the length l = 1.0 cm, the cross-sectional area A_w and the heat-conduction coefficient of stainless steel $K_{ss} = 1.45 \times 10^4 \times T$ erg/cm s K (Haasbroek [30]). The contribution $\dot{Q}_w$ is listed in table II. The contribution of the powder $\dot{Q}_p$ is very likely negligible compared to the contributions $\dot{Q}_l$ of the liquid and $\dot{Q}_w$ of the wall. In this approximation, the heat transported by the liquid can be calculated from $\dot{Q}_l = \dot{Q}_{wpl} - \dot{Q}_w$. The values of $\dot{Q}_l$ obtained in this way are also listed in table II.

The strong dependence of $\dot{Q}_l$ on T ($\simeq 12^{th}$ power) suggests that the heat is transported by the normal fluid flowing through the superleak. This

Table II

Heat conduction by the superleak.

T	$\dot{Q}_{wpl}/\Delta T$	$\dot{Q}_w/\Delta T$	$\dot{Q}_l/\Delta T$	Nr^4	r	λ
K	10^3erg/sK	10^3erg/sK	10^3erg/sK	10^{-12}cm^4	10^{-6}cm	10^{-7}cm
1.20	1.25	1.01	0.24	1.55	8.6	5.9
1.25	1.54	1.05	0.49	1.72	9.1	8.5
1.50	6.65	1.26	5.39	1.50	8.5	5.0
1.70	24.0	1.43	22.6	1.27	7.8	1.3
1.90	82.0	1.60	80.4	1.19	7.5	—

For definitions of symbols see text.

may be understood from the following arguments. If heat is transported through N parallel circular channels of radius r and length l, the mean velocity of the normal fluid in the channels is related to the heat current $\dot{Q}$ by:

$$v_n = \frac{\dot{Q}}{N\pi r^2 \rho S T} . \tag{3.2}$$

In subcritical flow, a Poiseuille pressure drop over the capillary leads to

$$\dot{Q} = \frac{\rho^2 S^2 T}{\eta_n} \frac{N\pi r^4}{8l} \Delta T . \tag{3.3}$$

The first factor is roughly proportional to T^{12}. It is tempting to compare the $\dot{Q}_l$, calculated from this experiment, with the $\dot{Q}$ of equation (3.3). From such a comparison, a value of Nr^4 can be obtained (see table II). Van Alphen et al. [31] were able to determine the mean open cross sections of their superleaks, from their experiments with the persistatron: 21 % and 28 % (see table I of ref.[31]). From their results, the mean open cross section of our superleak can be estimated to be 25 %

of the total cross section: $N\pi r^2 = 6.6 \times 10^{-2} cm^2$. Combining this relation with the value of Nr^4, the radii of the channels can be calculated (see table II). The radii r appear to be temperature dependent, since in these narrow channels ($d \simeq 1.5 \times 10^{-5}$cm), mean free path effects have to be taken into account. Therefore the linear Maxwell slip coefficient λ has to be introduced into the calculations (Brewer and Edwards [17], Cornelissen [32]). A correction with this slip coefficient is less important at high temperatures, so that the value of $r = 0.75 \times 10^{-5}$cm is the most reliable. Inserting this value of r into the data at lower temperatures, the slip coefficients λ are calculated (last column of table II). The slip coefficients obtained in this way are very close to the roton mean free paths (Atkins [33]), as should be expected. The number of channels is found to be 4×10^8.

In conclusion, it can be stated that heat is transported through a superleak filled with liquid helium by a laminar flow of the normal fluid. The agreement between the theoretical and experimental temperature dependence of the heat current is very good. Though a superleak certainly does not consist of parallel, circular channels, this simple physical picture may be helpful for a good understanding of the phenomena that are important in the case of heat transfer through a superleak. The results of the calculations of the number and radii of the circular channels are only to be considered as indications of the order of magnitude of the real channels in the superleak.

At the same time, but independent of this work, Van Spronsen et al.[34] also studied the heat transport through a superleak. Their results agree very well with the results of this experiment.

3-2. *Filmflow*. Except with NRS flow, the experimental apparatus is partially filled with liquid helium, and the walls at the upper part of the flow circuit will be covered by a liquid film of helium. During most of the measuring runs, the chemical-potential drop over the capillary has a non-zero value. As the chemical-potential drop over the superleak S_2 is always zero, the value of $\rho\Delta\mu$ found over the capillary equals that over the helium film. The gradient of the chemical potential acts as a driving force on the superfluid, so there will be a flowing film as soon as $\rho\Delta\mu$

is non-zero. This flowing film causes a transfer of mass, which results in the necessity of a correction to the superfluid velocity in the capillary. In order to minimize this correction, a film constriction is placed in the gas link. The film constrictions used are of diameter of 0.15 and 0.05 cm, in combination with the wide and narrow capillary, respectively. The film constrictions cannot be chosen arbitrarily small, because of the pressure difference caused by the gas flowing through the constriction. The amount of helium transported by the film has been measured with the capillary removed from the apparatus. The film-transfer rate determined in this way causes a correction to v_s of 0.2 cm/s in the wide capillary and of 0.7 cm/s in the narrow one.

From various experiments on film flow, it is known that reproducible film flows only can be obtained with clean surfaces. Since no special precautions were taken, it is not surprising that the measured transfer rate is a factor 4 greater than the very low transfer rate reported by Hebert et al. [35]. Very recently, Harris-Lowe and Turkington [36] reported film-transfer rates which depended on the chemical-potential difference in a very complex way.

We are not able to determine the film-transfer rate during the measuring runs with the capillary in the circuit. Because of these uncertainties, in all the values of v_s that will be quoted this correction has not been applied. In relevant cases, a possible film-flow correction will be considered in the discussion of the results.

3-3. *Kinetic energy.* From classical hydrodynamics, the kinetic-energy correction for a viscous fluid flowing out of a large tank through a pipe is known. The following contributions have to be considered:

1) If the velocity in the tank is negligible with respect to the mean velocity in the pipe $\bar{v}$, there exists a Bernoulli pressure drop $\frac{1}{2}\rho\bar{v}^2$.

2a) For laminar flow in a pipe, a parabolic velocity profile has to build up, giving rise to an additional pressure drop of $\frac{1}{2}\rho\bar{v}^2$.

2b) In the case of turbulent flow, the velocity profile is less pronounced than in the laminar case, resulting in an empirical pressure drop of approximately $0.045\rho\bar{v}^2$ (Prandtl & Tietjens [37]).

3) If the pipe has an entrance that is not rounded off, a vena contracta

takes place. The contracted jet expands to the full pipe radius, within a short distance, causing an additional pressure drop. This pressure drop varies from $\frac{1}{2}\rho\bar{v}^2$ to $\rho\bar{v}^2$, depending on the location of the entrance of the pipe with respect to the wall (Bayley [38]).

Combining these contributions for classical viscous fluids, one obtains kinetic-energy pressure drops of 1.0 - 2.0 $\rho\bar{v}^2$ in the case of laminar flow and of 0.55 - 1.55 $\rho\bar{v}^2$ for turbulent flow.

Analogous pressure drops are to be expected in experiments with helium II flowing through a capillary. If both components are flowing, one might expect two additional pressure drops, proportional to $\rho_s\bar{v}_s^2$ and $\rho_n\bar{v}_n^2$. In his isothermal flow experiments, using rounded-off entrances Atkins [23] has measured kinetic-energy pressure drops of 1.0 $\rho\bar{v}^2$. In the present experiments, a larger contribution can be expected, because of the sharp-edged entrances and the location of the entrance of the capillary in the liquid.

For laminar normal fluid flow through our capillary, with mean velocity v_n a kinetic-energy pressure drop in the range of 1.5 -2.0 $\rho_n v_n^2$ may be present. Since ρ_n is small at low temperatures, this term will only be detectable at high velocities. From measuring runs at T = 1.20 K and T = 1.25 K with v_n's up to 50 cm/s, the kinetic-energy pressure drop is determined to be 1.6 $\rho_n v_n^2$ (see section 4-1).

The motion of the excitations, produced by the energy dissipation of the normal fluid in the wide capillary, contributes 0.12 $\rho_n v_n^2$ at T is 1.20 K and 0.07 $\rho_n v_n^2$ at T is 1.25 K, and can therefore be neglected.

As was mentioned already in the introduction, superfluid helium flowing with a velocity above the critical velocity may be described by assuming the flow to be turbulent. Therefore it is likely that in this case, a kinetic-energy pressure drop of the order of 1.0 $\rho_s v_s^2$ applies. These pressure drops have to be subtracted from the ΔP's as derived in section 2-3, in order to obtain the pressure drops caused by the flow resistances. In all the relevant cases, these corrections will be considered.

A kinetic-energy pressure drop has also been observed across the film constriction in the gas. This constriction is a circular hole in a wall of only 0.05 cm thickness. In such a short "tube", only a kinetic-energy pressure drop is to be expected. The pressure drop over the constriction

is not the only pressure drop at the upper part of the apparatus. From the measured temperature difference $T_1 - T_4$, the corresponding pressure difference $P_1 - P_4$ has been calculated (see fig. 3). With the film constriction of diameter 0.15 cm, the pressure drop over the gas may be described with one relation at different temperatures, i.e.

$$P_1 - P_4 = \alpha T^{\frac{1}{2}} \rho_g \bar{v}_g + 1.6 \rho_g \bar{v}_g^2 \qquad (3.4)$$

with ρ_g the density of the gas, $\bar{v}_g$ the mean velocity of the gas in the film constriction, and α a constant ($\simeq 740$ cms^{-1} K$^{-\frac{1}{2}}$). Again a kinetic-energy pressure drop is significant: $1.6\, \rho_g \bar{v}_g^2$. The two contributions are of the same order of magnitude.

The first term on the right-hand side of eq.(3.4) represents the evaporation pressure drop ΔP_v. From simple kinetic arguments, Atkins [23] derived a pressure drop ΔP_v between an evaporating liquid and the gas above it

$$\Delta P_v = (4\dot{m}/A_v)(RT/3M)^{\frac{1}{2}}, \qquad (3.5)$$

with $\dot{m}$ the rate of evaporation, A_v the cross section of the surface of the evaporating liquid, R the gas constant and M the molecular weight. In the present case $A_v = 0.125$ cm^2. The rate of evaporation can be calculated from eq. (2.1a). On the condensation side, a similar pressure drop occurs, but since the surface of condensation is 2.8 cm^2, that pressure drop may be neglected. The pressure drop calculated from eq. (3.5) comes out to be a factor 2 larger than the experimental term $\alpha T^{\frac{1}{2}} \rho_g \bar{v}_g$. This discrepancy is probably caused by the curved evaporation surface, which may be twice the area calculated from the cross section of the tube (diam. 0.4 cm).

The pressure drop $P_1 - P_4$ has nothing to do with the situation in the capillary, but since it has an effect on the heights of the helium levels, it influences the limitation of the velocities which can be studied.

3-4. *Variation of T and S along the capillary.* In section 2-2, the calculation of the velocities is shown. In that section, the temperature and other thermodynamic quantities along the capillary are assumed to be

constant. In practice, a temperature difference over the capillary nearly always appears. As the entropy S strongly depends on temperature, the normal fluid velocity will not be the same at the entrance and the exit of the capillary. Therefore in all our measuring runs, an averaged v_n is calculated, using eq. (2.2a) or (2.2b), but inserting for S and T values averaged over the length of the capillary. All the values of v_n quoted are averaged in this way, as well as over the cross-sectional area. A correction on v_s with respect to the temperature drop over the capillary may be neglected. The fountain pressure drop over the capillary $\rho S\Delta T$ also is calculated using an average value for the entropy. These approximations are sufficiently accurate as long as the temperature drop is not too large.

With NRS flow, very high values of v_n are accompanied by large values of ΔT. For that reason, the fountain pressure drop over the capillary for NRS flow has to be computed from

$$\Delta P = \rho \int_{T_2}^{T_1} S(T)\,dT,$$

with T_1 and T_2 the temperatures at the two ends of the capillary.

4. Experimental results with small v_s.

Measuring runs are performed at selected temperatures. In this way, results from different types of flow taken at the same temperature can be compared. Most of the measuring runs are carried out at T is 1.20 K, 1.25 K, and 1.35 K. At T is 1.50 K, 1.70 K, and 1.90 K only a few series are measured. The results of the measuring runs in the region around the line $v_s = 0$ (see fig. 2) differ from the results obtained in other parts of the velocity plane. These measurements will therefore be treated first.

The presentation is divided into the following parts:

a) In section 4-1, the results of those measurements for which $\rho\Delta\mu = 0$ and therefore $\Delta P = \rho S\Delta T$ are treated. This part is called the linear region, because of the linear dependence of ΔT on the heat current.

b) In section 4-2 the results with $\rho\Delta\mu \neq 0$ and $\Delta P \neq \rho S\Delta T$ are presented, this is called the turbulent region.

c) In section 4-3 the results are compared with those of other experiments.

4-1. *Flow with small v_s, the linear region.* If heat is transported by a normal fluid flow through a circular capillary of radius r and length l, the normal fluid velocity v_n is related to the heat current $\dot{Q}$ by

$$v_n = \frac{\dot{Q}}{\pi r^2 \rho S T} . \tag{4.1}$$

A laminar flow of the normal component causes a pressure drop ΔP over the capillary according to Poiseuille's law,

$$\Delta P = - \frac{8\eta_n l}{r^2} v_n . \tag{4.2}$$

If $\dot{Q}$ is sufficiently small, the chemical-potential drop equals zero, and

$$\Delta P = \rho S \Delta T . \tag{4.3}$$

Combining these three equations a linear dependence on $\dot{Q}$ of the measured ΔT is found,

$$\rho S \Delta T = - \frac{8\eta_n l}{\pi r^4} \frac{\dot{Q}}{\rho S T} . \tag{4.4}$$

Eq.(4.4) also holds, as long as the condition (4.3) is satisfied, if there is a simultaneous flow of superfluid through the capillary.

In order to calculate a value for the viscosity from measurements on the temperature difference ΔT created by normal fluid flow through a capillary, the variations of S, η_n and T along the capillary have to be taken into account. In this way one obtains the relation

$$\frac{\Delta T}{\dot{Q}} = - \frac{8\eta_n l}{\pi r^4} \frac{T}{(\rho S T)^2} \left[1 - \frac{1}{2} \left(\frac{2}{\rho S T} \frac{\partial (\rho S T)}{\partial T} - \frac{1}{\eta_n} \frac{\partial \eta_n}{\partial T} - \frac{1}{T} \right) \Delta T \right] . \tag{4.5}$$

For small values of ΔT eq.(4.5) reduces to eq.(4.4). Brewer and Edwards [17] have derived nearly the same formula. They neglected the last term $(1/T)(\Delta T)$. However, as $1/T$ nearly equals $(1/\eta_n)(\partial \eta_n / \partial T)$, this omission

Fig. 5

The pressure drop over the capillary as a function of the normal fluid velocity. The straight line is calculated from eq. (4.2).

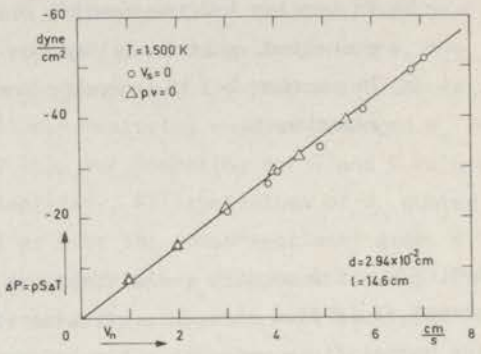

seems unwarranted.

With the present apparatus the linear region is studied in three different ways:

a) with no net mass flow as long as the superfluid flows subcritically, $\rho v = 0$;

b) with only the normal fluid flowing, $v_s = 0$ (the counterflow of superfluid is balanced);

c) with NRS flow.

Ad a). If $\rho v = 0$, the results show the usual pattern as illustrated in fig. 5. At low values of v_n, the pressure drop equals the expected Poiseuille pressure drop of eq. (4.2) and $\rho\Delta\mu$ equals zero. The limit of the linear region depends on temperature. At high temperatures, a critical value of v_s is already obtained at low values of v_n.

Ad b). A typical example of normal fluid flow without a superfluid counterflow, $v_s = 0$, is also shown in fig. 5. Within the measuring accuracy, the value of $\rho\Delta\mu$ is zero. The straight line in fig. 5 is the theoretical one, calculated from eq. (4.2) with $\eta_n = 13.55$ μP. Turbulent points have been omitted, as they drop out of scale.

At $T = 1.90$ K and $d = 0.95 \times 10^{-2}$ cm, measurements on flows with $\rho v = 0$ and $v_s = 0$ indicate clearly a difference in the creation of turbulence, which is caused by the simultaneous flow of the superfluid in the case of no net mass flow. With $v_s = 0$, the linear region reaches up to $v_n = 10$ cm/s, while with $\rho v = 0$ the upper limit is $v_n = 4.5$ cm/s, accompanied by $v_s = -2.8$ cm/s.

Ad c). In the type of flow called NRS flow, only the velocity of the

normal fluid in the capillary is known, and $\rho\Delta\mu$ has to be zero (see section 2-5). From our measurements with adjustable v_s and v_n (with a partly filled apparatus), it is known that flows with $\rho\Delta\mu = 0$ and $\Delta P = \Delta P_{Pois}$ are only possible in the immediate vicinity of the $v_s = 0$ and $\rho v = 0$ lines in the velocity diagram (fig. 2). This is in contradiction to the assumption of Staas et al.[22] in their original paper. They suggested that both in the laminar and turbulent situation, the superfluid and the normal fluid should move in the same direction, such that no effective mutual friction occurred. Our measurements indicate indeed that in the turbulent situation the superfluid moves with a velocity v_s slightly smaller than v_n. We shall come back to this type of flow in a following chapter. However, Staas' assumption seems not to be valid in the laminar situation. A laminar NRS flow may be identical to a no net mass flow or a pure normal fluid flow. It should be noted that in both situations the relative velocity may be very large. We observed laminar NRS flows with values of v_n up to 54 cm/s at $T = 1.20$ K in the wide capillary.

In fig. 6 the pressure drop over the capillary is plotted as a function of v_n, at $T = 1.20$ K for an NRS flow series. The solid line through zero represents the laminar normal flow. The measuring points shown above this line are turbulent points. The hysteresis in this type of flow will be discussed in a following chapter on turbulent flows with $v_s >> 0$. From

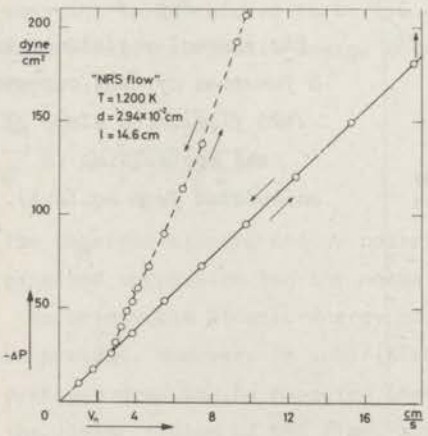

Fig. 6
The pressure drop over the capillary as a function of the normal fluid velocity in the type of flow called NRS *flow.*

Fig. 7

The thermal resistance as a function of heat current (NRS flow). The slope of the solid line is calculated from eq.(4.5).

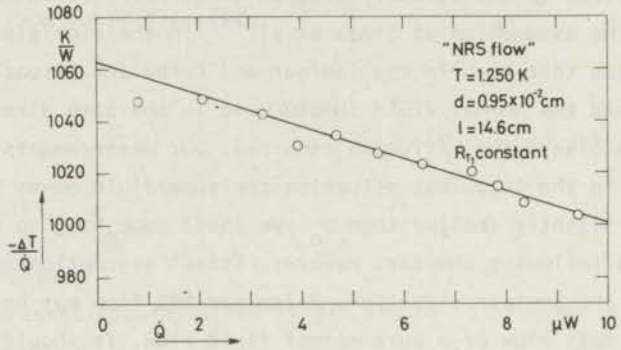

the solid line, the viscosity η_n can be deduced.

With the narrow capillary, the correction term in eq.(4.5), taking into account the variation of S, η_n and T along the capillary, is already significant at low heat currents, as shown in fig. 7. The slope of the solid line is calculated from eq.(4.5). From the intersection of this line with the vertical axis, the viscosity η_n is calculated. The

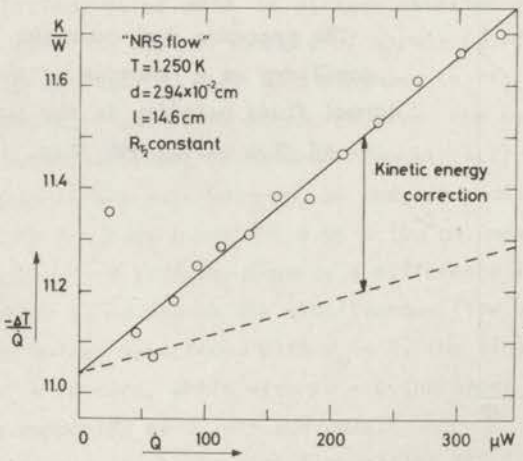

Fig. 8

The thermal resistance as a function of heat current (NRS flow). The slope of the dotted line is calculated from eq.(4.5).

Table III

Values of the viscosity η_n *computed from laminar* NRS *flow.*

T(K)	1.20	1.25	1.30	1.35	1.45	1.50	accuracy
η_n(μP)	17.8	16.4	15.6	15.0	14.0	13.5	$\pm$ 0.2

viscosities η_n, computed from measurements in the linear region of a great number of NRS flow series, are listed in table III. The results agree very well with the values listed in table I. At higher temperatures, T = 1.70 K and T = 1.90 K, the linear region is too small to give sufficient accuracy for a determination of η_n, but the results are not in contradiction with the values from table I.

The maximum velocity v_n obtained with linear flow in the series of fig.7 is 10.6 cm/s. In the wide capillary, linear flow is observed at still higher velocities. In fig. 8, the thermal resistance at T = 1.25 K in the wide capillary is shown (NRS flow). There is a large discrepancy between the experimental points and the dotted line calculated from eq.(4.5). The explanation of this discrepancy was already mentioned in section 3-3. At these high velocities a kinetic-energy correction proportional to $\rho_n v_n^2$ has to be applied. From graphs such as fig. 8, the proportionality constant is calculated to be 1.6 $\pm$ 0.1. The extra thermal resistance, describing the kinetic-energy correction, which has to be added to eq. (4.5) is

$$\frac{\Delta T}{\dot{Q}} = 1.6 \frac{\rho_n \dot{Q}}{\pi^2 r^4 \rho^3 S^3 T^2} . \qquad (4.6)$$

The observed kinetic-energy contribution lies within the limits of the expected correction for the normal fluid (section 3-3).

No observable kinetic-energy correction from the superfluid seems to be present. However, in subcritical superfluid flow, no kinetic-energy pressure drop may be expected (Meservey [39], Van Alphen et al.[31]). In the linear region of NRS flow, a possible superfluid flow is always subcritical, as $\rho\Delta\mu$ = 0 and $\Delta P = \Delta P_{Pois}$. If in this linear region the

superfluid should move with nearly the same velocity as the normal fluid, as Staas [22] assumed, subcritical superfluid flow with velocities up to 50 cm/s should have been present, which is very unlikely.

4-2. *Flow with small v_s, the turbulent region.* In the linear region, a possible flow of the superfluid is subcritical. The chemical-potential drop is zero, while the pressure drop equals the pressure drop created by the normal fluid according to Poiseuille's law (4.2). In the turbulent region, where $\rho\Delta\mu \neq 0$, the superfluid is supposed to be turbulent, and interacts with the normal fluid. The turbulent situation is studied in this section, in measuring runs with $v_s = 0$ or $\rho v = 0$.

A typical illustration of a measuring series on pure heat transport ($\rho v = 0$) is shown in fig. 9. Linear laminar flow is observed with velocities up to $v_n = 11.7$ cm/s, and corresponding $v_s = -0.8$ cm/s. In this laminar flow, $\rho\Delta\mu = 0$, and the pressure difference ΔP fits eq.(4.2). At a normal fluid velocity of 12.0 cm/s, the flow begins to become

Fig. 9

Result of a pure heat conduction flow experiment ($\rho v = 0$). The fountain pressure $\rho S\Delta T$, the chemical-potential difference $\rho\Delta\mu$ and the pressure difference ΔP are shown as functions of the normal fluid velocity v_n. For details see text.

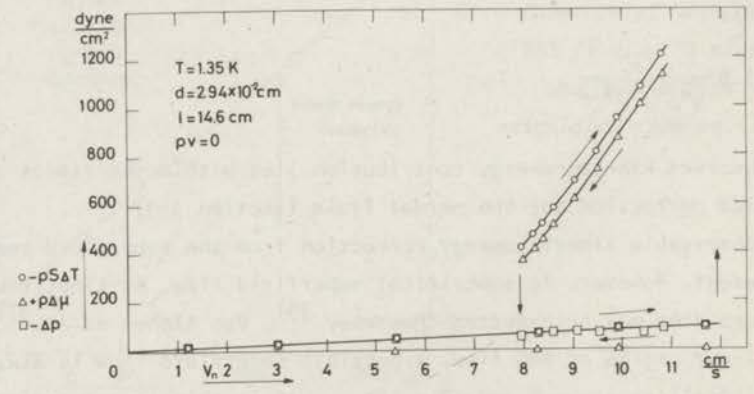

Fig. 10

The pressure drop over the capillary as a function of the velocity of the normal fluid v_n (no net mass flow). The circles represent linear flow, the squares turbulent flow. The dotted line is calculated from equation (4.8). $d = 2.94 \times 10^{-2}$ cm.

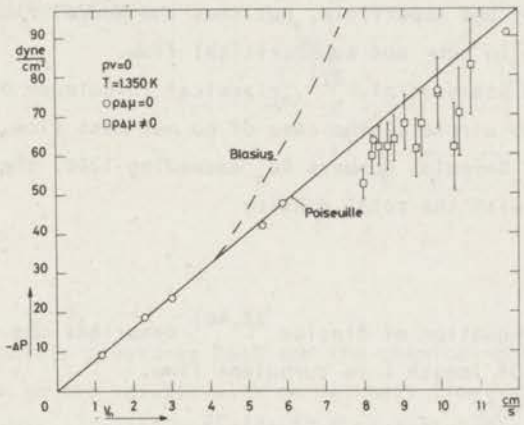

turbulent ($\rho\Delta\mu \neq 0$). This turbulent point can not be measured, since the helium level h_1 (see fig. 1) becomes too low. Once the flowing superfluid helium has a turbulent character, it remains turbulent if the velocities v_n and v_s are lowered. This turbulent part, however, does not reach down to the linear part: at v_n = 8.0 cm/s (v_s = -0.6 cm/s), the flow in the capillary does not remain turbulent for long, but drops to the laminar part, after having been turbulent for 5 minutes. The hysteresis in this type of flow is indicated also in fig. 9. However, the observed pressure drops show the same dependence on v_n, within the measuring accuracy, both in linear and in turbulent flow. This is illustrated more clearly in fig. 10. The error bars indicate the accuracy. These error bars are large, since the pressure drop ($\Delta P = \rho S \Delta T + \rho\Delta\mu$) is calculated from the difference of two large quantities, as shown in fig. 9. The fully drawn line is calculated according to eq.(4.2).

From ordinary hydrodynamics, it is known that the velocity profile of a viscous fluid flowing through a tube is directly related to the pressure drop over the tube (ignoring kinetic-energy effects). The same can be expected for a flow of the normal component of helium through a capillary. In the present experiment the observed pressure drops over the capillary for subcritical and for turbulent flow are always in accordance with Poiseuille's law. This suggests that the velocity profile of the normal fluid is not altered by the interaction of the normal fluid with the vortices of the superfluid, but that the normal fluid is moving laminarly both in sub- and supercritical flow.

According to Staas et al. [22], classical turbulence of the normal fluid might also play a role in the case of no net mass flow. Turbulence should be possible at Reynolds numbers Re_v exceeding 1200, these Reynolds numbers being defined with the *total* density

$$Re_v = \frac{\rho v_n d}{\eta_n} . \qquad (4.7)$$

The empirical equation of Blasius [22,40] describes the pressure drop across a tube of length l in turbulent flow.

$$\Delta P(\text{Blasius}) = \frac{4\eta_n^2 l}{\rho r^3} \times 4.94 \times 10^{-3}\, Re_v^{1.75} \quad \text{(c.g.s. units)}. \qquad (4.8)$$

In fig. 10, the pressure drop calculated from equation (4.8) is given by the dotted line. At T is 1.35 K, Re_v equals 1200 at v_n is 4.2 cm/s, in the capillary with diameter $d = 2.94 \times 10^{-2}$cm. As may be concluded from fig. 10, the observed pressure differences show the same dependence on v_n above and below $Re_v = 1200$. Even at $v_n = 10.8$ cm/s ($Re_v = 3100$), with a large chemical-potential difference present, the measured pressure drop does not indicate any turbulence of the normal fluid.

Usually, attempts to create turbulent flow with only the normal fluid moving are only successful when a vibration of the cryostat is first induced by tapping its top. An example of a measuring run with $v_s = 0$ is shown in fig. 11. The error bars indicate the accuracy. The solid line describes the pressure drop according to Poiseuille's law, eq.(4.2). As may be seen from fig. 11, the measured pressure drops at the turbulent measuring points still equal the pressure drops calculated from Poiseuille's law. This does not differ from the results obtained with no net mass flow.

Fig. 11

The pressure drop over the capillary as a function of the normal fluid velocity v_n. In this series, the superfluid velocity $v_s = 0$. The circles represent linear flow, the squares turbulent flow.

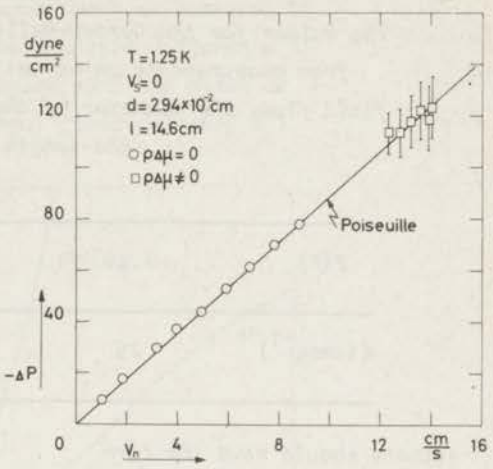

The observed fountain pressures $\rho S \Delta T$ and the chemical-potential drops $\rho \Delta \mu$ are very similar to the results with no net mass flow shown in fig. 9. This indicates that a small counterflow of superfluid is not important. From the observed pressure drops, the conclusion can again be drawn that the normal fluid is always flowing laminarly through the capillary with a parabolic Poiseuille profile.

As has been mentioned, it is difficult to create turbulence with only the normal fluid moving. However, though the normal fluid flows laminarly, the superfluid can be turbulent, in spite of the requirement that the mean superfluid velocity is zero. It should be remembered again, that in the present experiment, only the macroscopic mean values of the velocities, averaged over the capillary are known.

In order to describe the experimental results for stationary flow, two new quantities F_{sn} and F_s' are defined with the following equations:

$$0 = -\rho_s \frac{\Delta\mu}{l} - F_{sn} - F_s', \tag{4.9}$$

$$0 = -\rho_n \frac{\Delta\mu}{l} - \rho S \frac{\Delta T}{l} + F_{sn} - F_n. \tag{4.10}$$

F_n is the normal viscous force. F_{sn} corresponds to the mutual friction force introduced by Gorter and Mellink [9], which according to these

Table IV

The values for the Gorter–Mellink constant A, as calculated from measurements on no net mass flow and pure normal fluid flow. The diameter of the capillary is 2.94 x 10^{-2} cm, the length 14.6 cm.

T(K)	1.20	1.25	1.35	1.50
A(cmsg^{-1})	25	33	39	47

authors should have the form

$$F_{sn} = A\rho_s\rho_n (v_s - v_n)^3. \qquad (4.11)$$

As can be seen easily by adding eqs. (4.9), and (4.10),

$$\Delta P = - lF_n - lF'_s .$$

During the measuring runs with small v_s, reported in this chapter, F'_s is always zero within the measuring accuracy, since the observed pressure difference equals the Poiseuille difference caused by the moving normal liquid (eq. (4.2)).

Values for the Gorter-Mellink constant A, concluded from the present measurements on no net mass flow and pure normal fluid flow through the wide capillary, are the same within the measuring accuracy. These values are listed in table IV. The values of A are somewhat higher than the values found by Vinen [10] and Wiarda and Kramers [26,27], but slightly less than the values obtained by Brewer and Edwards [20]. As will be shown in a following chapter, A-values from other measuring runs, with other velocity combinations (v_n, v_s), are not the same as the values obtained from no net mass flow experiments.

4-3. *Comparison with other experiments.* There are only a few experiments on heat flow through a capillary in which the pressure differences ΔP have been measured. Brewer and Edwards [19] (BE) have observed pressure and temperature differences in no net mass flow through a capillary of

Fig. 12

Result of a heat-flow experiment as measured by Brewer and Edwards. The pressure difference ΔP and the fountain pressure $\rho S \Delta T$ are shown as functions of the normal fluid velocity v_n.

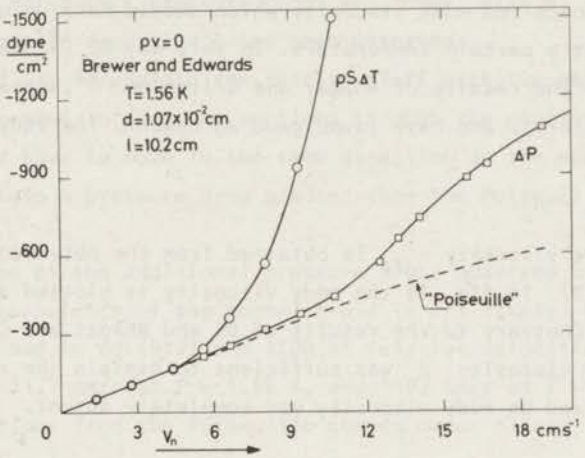

diameter 1.08×10^{-2}cm and length 10.2 cm. In fig. 12, their results at $T = 1.56$ K are shown as a function of the normal fluid velocity v_n. The values of v_n quoted in this figure are not averaged over the length of the capillary, but are the values of v_n at the cold end of the capillary. There are some striking differences between the results of the experiment of BE and the present experiment.

The first difference between the results shown in fig. 9 and fig. 12 concerns $\rho S \Delta T$. In the present experiment, the $\rho S \Delta T$ curve does not reach down to the ΔP curve. In fig. 12 the $\rho S \Delta T$ curve intersects the ΔP curve. BE [18] have observed such a behaviour in capillaries with diameters of 0.52×10^{-2}cm, 1.08×10^{-2}cm, and 3.66×10^{-2}cm. Therefore the disagreement between their results and ours is not caused by the difference in diameter. The gap in our experiment probably suggests that it is difficult to create or maintain turbulence in the capillary. A hysteresis as shown in fig. 9 was not reported by BE for the series of fig. 12. However, in ref. 18 they also mention hysteresis effects in other measuring runs with the same capillary.

The second important difference between our results and those of BE is

the dependence of ΔP on v_n in the turbulent region. In the present experiment (see fig. 10) the pressure drop over the capillary nearly equals the theoretical Poiseuille pressure drop. BE have observed pressure drops much greater than should be expected from Poiseuille's law.

For a comparison of these different experiments, it is perhaps useful to choose the so-called eddy viscosity which should be a unique function of $(v_n - v_s)d$ at a certain temperature. In this way BE [19] have compared their results with the results of Bhagat and Critchlow [11], obtained with a similar apparatus, and have found good agreement. The eddy viscosity is defined as

$$\eta_{eddy} = \eta_{eff} - \eta_n.$$

The effective viscosity η_{eff} is obtained from the observed pressure drop using eq.(4.2). In fig. 13 the eddy viscosity is plotted as a function of $(v_n - v_s)d$. Contrary to the results of BE and Bhagat and Critchlow [11], the ordinary viscosity η_n was sufficient to explain the results of our experiment, and an eddy viscosity was completely absent.

Fig. 13

The eddy viscosity as a function of $(v_n - v_s)d$ in no net mass flow. Fully drawn lines are measurements of Brewer and Edwards [19] ($d = 1.08 \times 10^{-2}$ cm). The dotted line is observed by Bhagat and Critchlow [11] ($d = 2.97 \times 10^{-2}$ cm). The measuring points are from the present research. ($d = 2.94 \times 10^{-2}$ cm, ○ : 1.50 K, Δ : 1.35 K, □: 1.20 K).

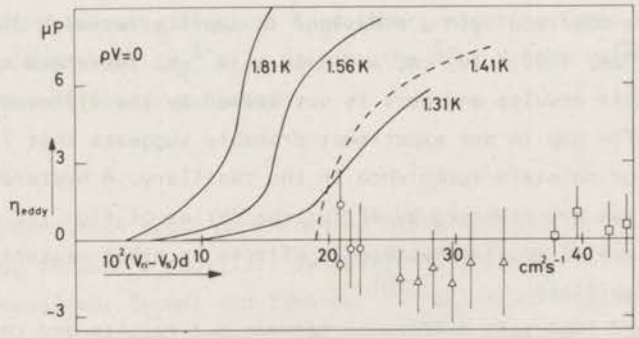

In a following chapter, however, measurements will be described in which a pressure drop over the capillary is observed with pure superfluid flow. Moreover, measuring runs will be reported in which the normal and superfluid (with $v_s >> 0$) move in opposite directions. In general, with these experiments in the counterflow region, only pressure drops smaller than the calculated Poiseuille pressure drops are found. With $v_n \simeq - v_s$ even flow with a pressure drop $\Delta P = 0$ has been observed.

If one should try to explain the results of BE with the help of an extra pressure drop needed to push the vortices through the capillary, the vortices should have to move in the same direction as the normal fluid, in order to obtain a pressure drop greater than the Poiseuille pressure drop.

An explanation of the additional pressure drops observed by BE, by means of a possible turbulence of the normal fluid is not likely. Reynolds numbers as defined in eq.(4.7) are 1200 at relative velocities of 12.6 cm/s at T = 1.31 K, 11.7 cm/s at T = 1.56 K, and 14.7 cm/s at T = 1.81 K. However, deviations from the Poiseuille curves occur already at lower values of $(v_n - v_s)$.

5. Conclusion.

In the turbulent region of no net mass flow, there is a strong interaction between the normal and superfluid, which can be concluded from the observed chemical-potential drops. The pressure drops equal the theoretical Poiseuille pressure drops, indicating that the normal fluid is moving laminarly both in sub- and supercritical flow. Until now, it is not clear what causes the difference in the observed pressure drops between our results and the results of Brewer and Edwards. The present results, however, seem to be the most simple ones. The difference in the results may perhaps be caused by different technical arrangements.

References

1) Van Alphen, W.M., De Bruyn Ouboter, R., Taconis, K.W. and De Haas, W., Physica 40 (1969)469 (Commun. Kamerlingh Onnes Lab., Leiden No.367a).
2) De Bruyn Ouboter, R., Taconis, K.W. and Van Alphen, W.M., Progress in low Temp. Phys., ed. C.J. Gorter, North-Holland Publ. Comp. (Amsterdam, 1967) Vol. V, chap.2.
3) Kidder, J.N. and Fairbank, W.M., Proc. of the 7th int. Conf. on low Temp. Phys., LT 7, eds. Graham and Hollis Hallett, North-Holland Publ. Comp. (Amsterdam, 1961) p. 560.
4) Peshkov, V.P. and Struykov, V.B., Soviet Physics-JETP 14(1962)1031.
5) Staas, F.A. and Taconis, K.W., Physica 27 (1961)924 (Commun. Kamerlingh Onnes Lab., Leiden No. 329b).
6) Olijhoek, J.F., Van Alphen, W.M., De Bruyn Ouboter, R. and Taconis, K.W., Physica 35(1967)483.
7) Kidder, J.N. and Blackstead, H.A., Proc. of the 9th int. Conf. on low Temp. Phys., LT 9, Plenum Press (New York, 1965) p.331.
8) Keller, W.E. and Hammel, E.F., Physics 2(1966)221.
9) Gorter, C.J. and Mellink, J.H., Physica 15(1949)285 (Commun. Kamerlingh Onnes Lab., Leiden, Suppl. No.98a).
10) Vinen, W.F., Proc. Roy. Soc. A240(1957)114 and 128, 242(1957)493, 243(1958)400.
11) Bhagat, S.M. and Critchlow, P.R., Cryogenics 2(1961)39.
12) Bhagat, S.M. and Critchlow, P.R., Canad. J. Phys. 41(1963)1307.
13) Bhagat, S.M., Critchlow, P.R. and Mendelssohn, K., Cryogenics 4(1964)166.
14) Peshkov, V.P. and Tkachenko, V.K., Soviet Physics-JETP 14(1962)1019.
15) Raja Gopal, E.S. and Tirmizi, S.M.A., Cryogenics 4(1964)378.
16) Chase, C.E., Phys. Rev. 127(1962)361.
17) Brewer, D.F. and Edwards, D.O., Proc. Roy. Soc. A251(1959)247.
18) Brewer, D.F. and Edwards, D.O., Phil. Mag. 6(1961)775.
19) Brewer, D.F. and Edwards, D.O., Phil. Mag. 6(1961)1173.
20) Brewer, D.F. and Edwards, D.O., Phil. Mag. 7(1962)721.
21) Alcaraz, E.C. and Madden, H.H., Phys. Rev. A3(1971)1698.
22) Staas, F.A., Taconis, K.W. and Van Alphen, W.M., Physica 27(1961)893 (Commun. Kamerlingh Onnes Lab., Leiden No.328d).
23) Atkins, K.R., Proc. Roy. Soc. A64(1951)833.

24) Bhagat, S.M. and Mendelssohn, K., Cryogenics 2(1961)34.
25) Wiarda, T.M., Van der Heijden, G. and Kramers, H.C., Proc. of the 9th int. Conf. on low Temp. Phys., LT 9, Plenum Press (New York, 1965) p.284.
26) Kramers, H.C., Superfluid Helium, ed. J.F. Allen, Academic Press (London and New York, 1966) p.199.
27) Wiarda, T.M., Thesis (Leiden, 1967).
28) Van der Heijden, G., Van der Boog, A.G.M. and Kramers, H.C., Proc. of the 12th int. Conf. on low Temp. Phys., LT 12, Academic Press of Japan (Tokyo, 1971) p.65.
29) Van Alphen, W.M., De Bruyn Ouboter, R., Olijhoek, J.F. and Taconis, K.W., Physica 40(1969)490 (Commun. Kamerlingh Onnes Lab., Leiden No.368a).
30) Haasbroek, J.N., Thesis (Leiden, 1971).
31) Van Alphen, W.M., De Bruyn Ouboter, R., Taconis, K.W. and Van Spronsen, E., Physica 39(1968)109 (Commun. Kamerlingh Onnes Lab., Leiden No. 366a).
32) Cornelissen, P.L.J. and Kramers, H.C., Proc. of the 9th int. Conf. on low Temp. Phys. LT 9, Plenum Press (New York, 1965) p.316.
33) Atkins, K.R., Liquid Helium, Cambridge University Press (London, 1959) p.109.
34) Van Spronsen, E. et al., private communication, to be published.
35) Hebert, G.R., Chopra, K.L. and Brown, J.B., Phys. Rev. 106(1957)391.
36) Harris-Lowe, R.F. and Turkington, R.R., J. of low Temp. Phys. 4(1971)525.
37) Prandtl, L. and Tietjens, O.G., Applied Hydro- and Aeromechanics, Dover Publications (New York, 1934) p.51.
38) Bayley, F.J., An introduction to Fluid Dynamics, George Allen and Unwin Ltd. (London, 1958) p.113.
39) Meservey, R., Phys. Fluids 8(1965)1209.
40) Schlichting, H., Boundary Layer Theory, Pergamon Press (London, 1955) p.401.

CHAPTER II

SUPERFLUID FLOW

Synopsis

Superfluid flow has been studied in two capillaries with diameters of 2.94×10^{-2} cm and 0.95×10^{-2} cm, at temperatures ranging from 1.2 K to 1.5 K. The chemical-potential difference and the temperature difference over the capillary are determined as a function of the superfluid velocity v_s. From these values the pressure drop over the capillary is derived. Curiously, for turbulent superfluid flow, the pressure drop resembles the classical pressure drop caused by a turbulently flowing ordinary liquid. There appears to be a connection between the pressure drop and the mutual friction, suggesting that both may be related to the vorticity in the superfluid.

1. Introduction

The aim of this research is to study the forces, acting on the superfluid and the normal fluid, in different types of flow through the same capillary. In a preceding chapter [1] (I), the experimental arrangements a) and b) were described, in which the two fluids can be forced to flow simultaneously through a capillary, with independently adjustable velocities. Studied were two stainless-steel capillaries of 2.94×10^{-2} cm and 0.95×10^{-2} cm, inner diameter, both 14.6 cm long. The manner in which the mean values of the velocities v_s and v_n, the chemical-potential difference $\rho\Delta\mu$, and the fountain pressure $\rho S\Delta T$ are obtained from the measurements is described in I. The pressure drop ΔP is calculated using the integrated thermodynamic identity, which for small ΔT and $\Delta\mu$ reads as

$$\Delta P = \rho S\Delta T + \rho\Delta\mu \ ; \qquad (1.1)$$

in this expression velocity contributions are neglected.

If $\rho\Delta\mu$ is not identically zero, the flow shall be called turbulent (supercritical), and will be discussed using the picture of vortex lines in the superfluid (Vinen [2]).

In order to describe the experimental results for stationary turbulent

flow in a capillary of length l, two quantities F_{sn} and F'_s are defined by the following equations:

$$0 = -\rho_s(\Delta\mu/l) - F_{sn} - F'_s , \tag{1.2}$$

$$0 = -\rho_n(\Delta\mu/l) - \rho S(\Delta T/l) + F_{sn} - F_n . \tag{1.3}$$

F_n is the normal viscous force. These equations resemble the equations of motion for stationary flow. However, since there is some uncertainty about the admissibility of inserting forces such as $\vec{F}_{sn}$ and $\vec{F}_s$ into the original equations of motion, it is preferable to introduce in this chapter averaged values F_{sn} and F'_s, since these are deduced directly from the experiments. All the terms in eqs. (1.2) and (1.3) have the dimension of a force per unit volume. In the calculations of the fountain pressure the mean value of S over the capillary is used. The force F_{sn} corresponds to the mutual friction force introduced by Gorter and Mellink [3], its analytical form, however, being unspecified for the time being.

By adding the eqs. (1.2) and (1.3), it follows that

$$\Delta P = -lF'_s - lF_n .$$

In chapter I experimental results for no net mass flow and for pure normal fluid flow ($v_s = 0$) were reported. In these types of flow the pressure drop obeys Poiseuille's law, both in sub- and supercritical flow, indicating that lF'_s is negligible in these cases and the normal fluid remains laminar.

In this chapter, II, results for superfluid flow will be presented. In these runs lF'_s is not negligible but lF_n is small (because of the inevitable heat leak through a superleak, a small normal fluid flow through the capillary may also be present). The quantity lF'_s includes, apart from the main term lF_s describing the pressure drop over the capillary, a kinetic-energy correction $\alpha\rho_s v_s^2$ originating from the entrance of the capillary. α can be estimated to be approximately 1.0 in the case of turbulent superfluid flow (see I-3-3). A similar correction to lF_n can be neglected since $\rho_n \ll \rho_s$ and v_n remains small in the runs with "pure" superfluid flow presented in this chapter. With these small values of v_n it is reasonable to use Poiseuille's law to calculate the pressure drop caused by the moving normal fluid. Therefore, lF_s can be obtained from

$$-lF_s = \Delta P + 1.0\ \rho_s v_s^2 + (8\eta_n l/r^2)\ v_n . \tag{1.4}$$

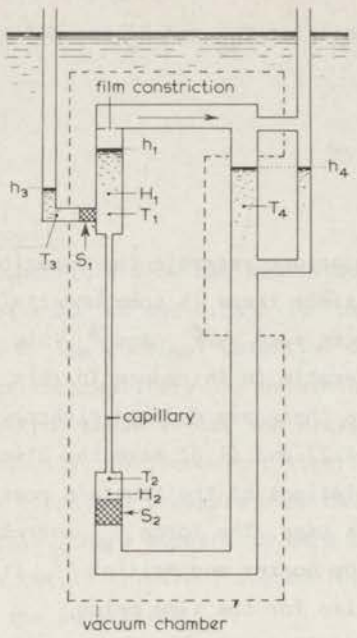

Fig. 1
Schematic drawing of the apparatus type a). (S)-Superleak; (H)-Heater; (T)-Thermometer; (h)-helium level.

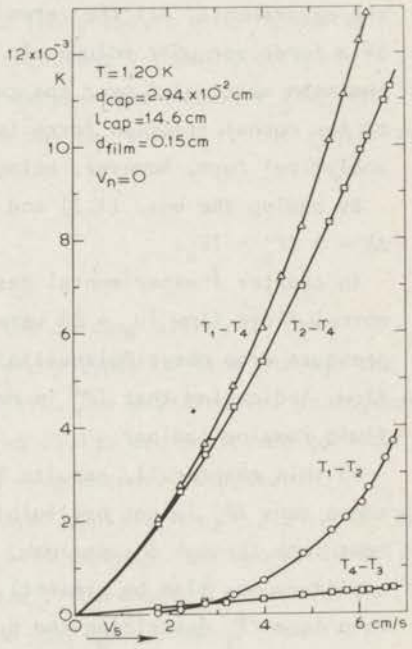

Fig. 2
Temperature differences observed with a pure superfluid flow as a function of the superfluid velocity v_s. For details see text.

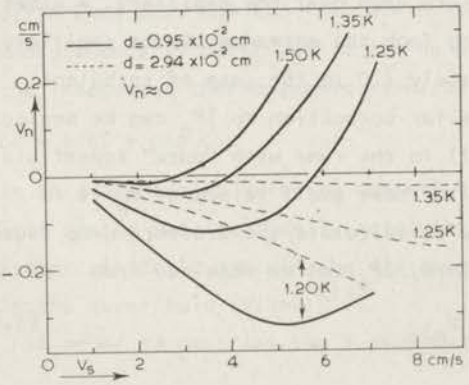

Fig. 3
The calculated values of the velocity v_n, of the small normal fluid flow caused by the heat leak through the superleak, as a function of the superfluid velocity v_s, at different temperatures.

The last term at the right-hand side of eq.(1.4) may give a noticeable correction with the narrow capillary, while with the wide capillary the kinetic-energy correction to ΔP rises to 10 % of ΔP at high values of the velocity v_s.

In the following chapter, III, results for types of flow in which both fluids move with velocities unequal to zero, shall be presented.

2. Superfluid flow, experimental results and discussion.

2-1. *General.* No systematic deviation between the results observed with the arrangements a) and b) has been found. Arrangement a) is shown schematically in fig. 1. Dissipation of heat in H_1 causes a distillation of helium resulting in a superfluid flow through the capillary. The velocity v_s is calculated from the power dissipated in H_1, and the heat of evaporation L together with the small correction ST, representing the mechanocaloric effect. In order to give an idea of the order of magnitude of the effects, an example of the temperature differences present between several parts of the apparatus type a) is shown in fig. 2. During this run the temperature T_1 was kept constant by adjusting the bath temperature. The temperature drop over the capillary $(T_1 - T_2)$ is caused by the superfluid flow in the capillary. The temperature drop over the gaslink is called $(T_1 - T_4)$ (see I-3-3). The temperature drop over the superleak S_2, $(T_2 - T_0) = (T_2 - T_4)$, causes a small heat leak through the superleak, and, therefore, a small normal fluid flow through the capillary (see I-3-1).

The temperature drop between the two glass standpipes, $(T_4 - T_3)$, is caused by the Kapitza resistance between the liquid in the apparatus and in the bath. It should be noted that at other temperatures than 1.2 K, and/or with other types of flow, the temperature drops in fig. 2 have entirely different values.

In fig. 3 the velocity of the small normal fluid flow calculated from the measured heat conduction of S_2, is shown for both capillaries. As could be expected this extra flow is more important for the narrow capillary than for the wide one. The heat leak through S_1 is negligible with respect to the heat dissipated in H_1.

Fig. 4

The chemical-potential drop $\rho\Delta\mu$, the fountain pressure $\rho S\Delta T$, and the pressure drop ΔP as functions of the superfluid velocity v_s for a "pure" superfluid flow.

a) narrow capillary *b) wide capillary*

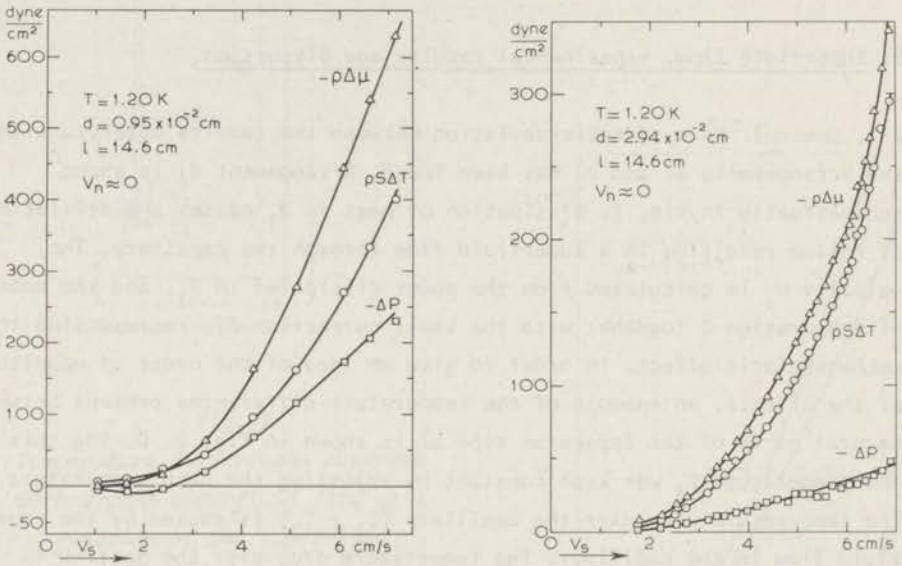

The behaviour of the chemical-potential, the temperature and the pressure drop over the capillaries, for a "pure" superfluid flow is illustrated in the figures 4a and 4b. In the narrow capillary the extra normal fluid flow is responsible for the initial dip of the ΔP curve. Apart from the mutual friction term, which in a superfluid flow is approximately given by $\rho S\Delta T$, the occurrence of a pressure difference ΔP observed in this type of flow is striking.

2-2. *Pressure drop*. The values of the uncorrected pressure drop over the capillaries are shown in the figures 5 and 6.
In fig. 5 (narrow capillary) the accuracy is 3 % of ΔP or 3 dyne/cm^2,

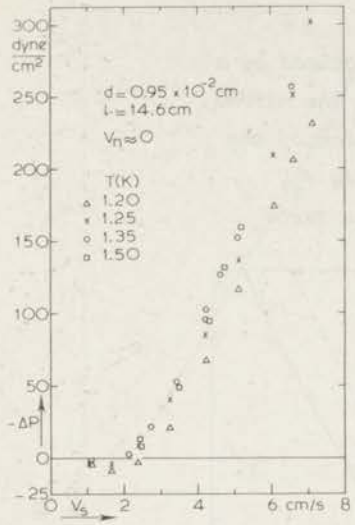

Fig. 5
The pressure drop ΔP over the narrow capillary as a function of the superfluid velocity v_s.

whatever the greatest. These pressure drops are smaller than the Poiseuille pressure drops ΔP_p observed with comparable normal fluid velocities ($\Delta P_p \simeq -80\, v_n$).
In fig. 6 (wide capillary) the accuracy is 10 % of ΔP or 3 dyne/cm^2. These pressure drops are comparable with Poiseuille pressure drops ($\simeq -8\, v_n$).

A typical example of the corrected pressure drop lF_s over the narrow capillary, calculated from the measurements using eq.(1.4), is shown in fig. 7 for T = 1.25 K. The solid line through the measuring points is the

Fig. 6
The pressure drop ΔP over the wide capillary as a function of the superfluid velocity v_s.

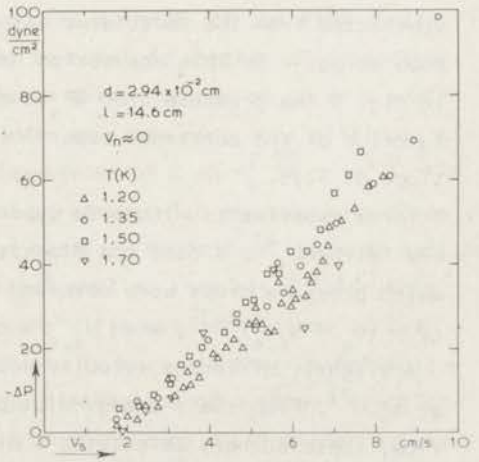

Fig. 7
The pressure drop lF_s, caused by a superfluid flow through the narrow capillary, as a function of the superfluid velocity v_s.
For dashed line see text.

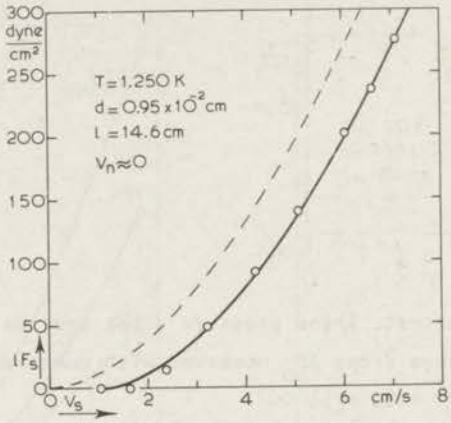

line $11.6(v_s - 1.0)^{1.75}$. The same dependence of lF_s on $(v_s - 1.0)^{1.75}$ is also found at T equal to 1.20, 1.35, and 1.50 K. As was mentioned already in I-3-2, a correction to v_s to account for the film transfer has to be applied as soon as $\rho\Delta\mu \neq 0$. This correction was estimated at 0.7 cm/s in the narrow and 0.3 cm/s in the wide capillary, and has to be subtracted from the calculated values of the superfluid velocity v_s as soon as $\rho\Delta\mu < 0$. This correction has not yet been applied in fig. 7. In fig. 8 the pressure drop lF_s over the wide capillary is plotted as a function of the corrected superfluid velocity. The line is drawn with a slope of 1.75.

Three experiments with pure superfluid flow are reported earlier (Kidder and Fairbank [4], Kidder and Blackstead [5], Keller and Hammel [6]), in which pressure drops were observed depending on the velocity as $\Delta P \sim (v_s - v_{s,c})^{1.75}$, with $v_{s,c}$ a critical velocity.

A slightly different velocity dependence has been found by Van Alphen et al. [7]. From their energy-dissipation measurements with pure superfluid flow, these authors calculated a dissipative pressure drop

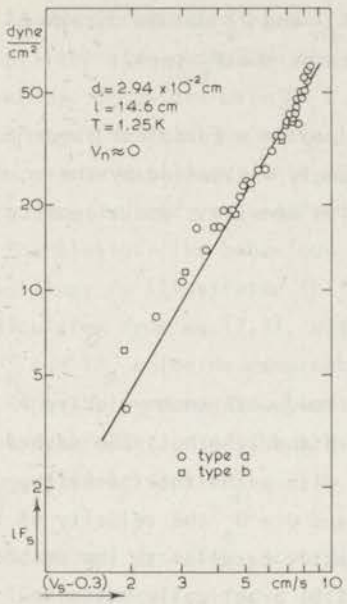

Fig. 8

The pressure drop $1F_s$ for superfluid flow through the wide capillary, as a function of the corrected superfluid velocity (v_s - 0.3). The circles are observed with arrangement a), the squares with arrangement b). (see I-2-1).

$$\Delta P_{dis} = \dot{E}/Ov_s \,, \tag{2.1}$$

with O the area of the chamber or slit, and $\dot{E}$ the observed energy dissipation. They found this dissipative pressure to depend on the velocity as

$$\Delta P_{dis} = \tfrac{1}{2}Bl v_s^2 \,, \tag{2.2}$$

with l the length of the flow path and B a phenomenological constant, depending on the temperature and on the diameter of the flow domain. It will be clear that it is difficult to conclude whether ΔP depends on $v_s^{1.75}$ or $v_s^{2.0}$, if one is only able to obtain values of ΔP in a small velocity region. In Van Alphen's case this was even more difficult since he had to distinguish between a dependence of $\dot{E}$ on $v_s^{2.75}$ or $v_s^{3.0}$. The B values of Van Alphen are in good agreement with the pressure drops in our narrow capillary. However, our pressure drops over the wide capillary yield a B value which is a factor 4-8 smaller than his B value.This discrepancy is probably caused by the different definitions of the pressure drops in their experiment and in ours. In their experiment a possible contribution to the energy dissipation of a mutual friction force F_{sn} could not be separated from the energy dissipation caused by a

frictional force F_s. From our experiments F_{sn} and F_s can be obtained separately, and our pressure drop only contains the F_s term.

Our preference to describe the pressure drop in a turbulent superfluid flow with a 1.75th power dependence is strongly influenced by the following similarity. In ordinary fluids with density ρ and viscosity η, the empirical relation of Blasius [8,9],

$$\frac{\Delta P_B}{l} = -\,0.158 \left[\frac{\rho^3 \eta^7 v^7}{d^5} \right]^{\frac{1}{4}} \qquad \text{(cgs units)}, \tag{2.3}$$

describes the pressure drop for turbulent flow, with mean velocity v through a circular capillary with diameter d and length l. The dashed line in fig. 7 is calculated from eq.(2.3) with ρ the total density, $\eta = \eta_n$ the viscosity of the normal fluid, and $v = v_s$ the velocity of the superfluid. The solid line in fig. 7 is exactly parallel to the dashed line. Insertion of ρ_s instead of ρ in eq.(2.3) practically makes no difference at these low temperatures. There is a small discrepancy between the estimated film correction of 0.7 cm/s, and the shift between the two lines in fig. 7 of 1.0 cm/s. This may be due to, either a wrong film-correction, or the presence of a $v_{s,c}$ of 0.3 cm/s as found in other experiments [4-6]. Apart from this shift the pressure drop lF_s in the narrow capillary is of the same magnitude as the classical pressure drop.

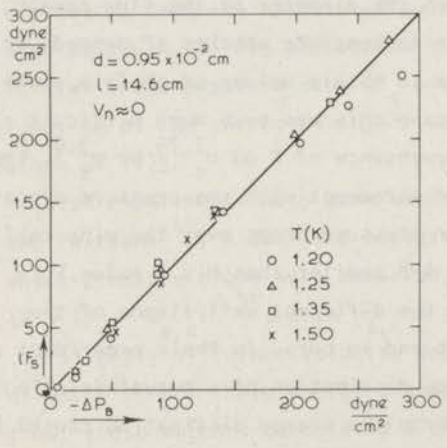

Fig. 9

The pressure drop lF_s, caused by a superfluid flow in the narrow capillary as a function of the pressure drop calculated from eq.(2.3).

As was illustrated already in fig. 8 the pressure drops over the wide capillary also depend on the 1.75th power of the velocity. However, these pressure drops are only 50 % of the pressure drops calculated from eq.(2.3). Although the relative measuring accuracy is smaller in the wide than in the narrow capillary, this difference is much larger than the claimed accuracy and not yet understood.

The Blasius-like behaviour of the pressure drop lF_s over the narrow capillary is illustrated in fig. 9. In this graph the values of ΔP_B are calculated from eq.(2.3), with the total density, $\eta = \eta_n$, and $v = v_s - 1.0$. ΔP_B and lF_s coincide remarkably well at all the observed temperatures.

A possible mechanism which might explain the essential role of η_n in the determination of the pressure drop caused by a superfluid flow, is suggested in section 4.

2-3. *Mutual friction.* According to the eqs. (1.2) and (1.3) the mutual friction force F_{sn} for a pure superfluid flow ($F_n = 0$), is defined by

$$F_{sn} = \rho_s S\,(\Delta T/l) + (\rho_n/\rho)(\Delta P/l). \qquad (2.4)$$

At low temperatures, where $\rho_n/\rho \ll 1$, the second term at the right-hand side of eq.(2.4) is small, as can be concluded from the figures 4a and 4b. Therefore, the dependence of $\rho S\Delta T$ on the relative velocity $(v_s - v_n)$, as shown in fig. 10, also illustrates the behaviour of F_{sn}. The velocities

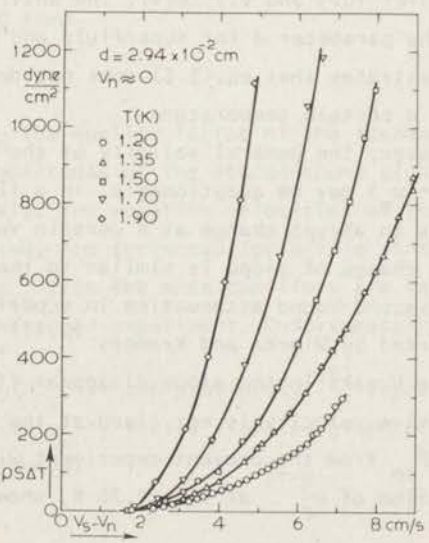

Fig. 10
The fountain pressure $\rho S\Delta T$ for "pure" superfluid flow as a function of $(v_s - v_n)$ at different temperatures.

are not corrected for a film contribution, which makes no appreciable difference. Values of $\mathcal{L}F_{sn}$ are calculated from the observed values of ΔT and $\rho\Delta\mu$, using eq.(1.3). Gorter and Mellink [3] have introduced a phenomenological form for F_{sn}

$$F_{sn} = A\,\rho_s\rho_n(v_s - v_n)^3, \tag{2.5}$$

with A depending on the temperature, which fitted the experimental data available at that moment (mainly from no net mass flow). As was shown by Wiarda and Kramers [10,11], the results of other types of flow could not be described with this equation for F_{sn}. However, in order to be able to compare results of different types of flow or different experiments it may be convenient to describe the results in values of A. This has been done in I for the results of no net mass flow, and is also possible for superfluid flow, since the values of $\mathcal{L}F_{sn}$ calculated from the present measurements are roughly proportional to the cube of the relative velocity. The values of A calculated for the wide capillary are (accuracy $\pm$ 5): 106, 89, 81, 76, 87, and 97 cm s/g for T equal to 1.20, 1.25, 1.35, 1.50, 1.70, and 1.90 K, respectively. In the narrow capillary the values of A are (accuracy $\pm$ 10): 148, 171, 154, and 132 cm s/g at T equal to 1.20, 1.25, 1.35, and 1.50 K, respectively. The quoted values of A are determined from double-logarithmic plots of $\mathcal{L}F_{sn}$ as a function of the relative velocity $v_r = v_s - v_n$. The values of v_r are corrected for the film transfer (0.3 and 0.7 cm/s). The entirely different temperature dependence of the parameter A for superfluid and no net mass flow (see I) clearly demomstrates that eq.(2.5) does not describe all types of flow with one A at a certain temperature.

Moreover, the general validity of the cubic dependence of F_{sn} on $(v_s - v_n)$ may be questionable. In a linear graph the slope of $\mathcal{L}F_{sn}$ on v_r^3 shows an abrupt change at a certain velocity at most of the temperatures. This change of slope is similar to the change of slope in the curves of the second-sound attenuation in superfluid flow as a function of v_r, as reported by Wiarda and Kramers [10,11], and by Le Ray et al. [13]. However, these breaks in the slope disappear if the dependence of $\mathcal{L}F_{sn}$ on the relative velocity is not fixed at the third power. For instance, a plot of $\mathcal{L}F_{sn}$ from the present experiment with the wide capillary, as a function of $v_r^{2.75}$ at T is 1.20 K, shows one straight line through all the

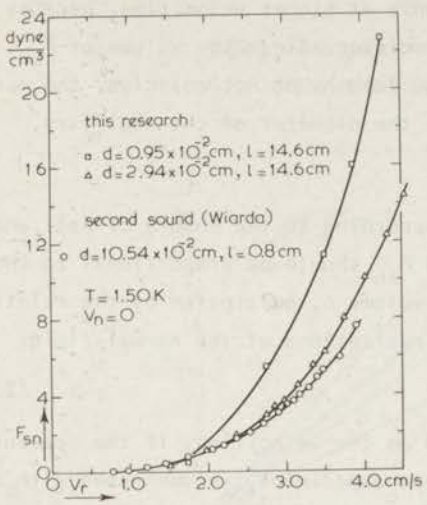

Fig. 11
Values of the mutual friction force F_{sn} calculated from the measurements of Wiarda and Kramers, together with values of F_{sn} from the present research, as a function of the relative velocity v_r.

measuring points. The results for F_{sn} from the present experiment can better be described with a power which slightly rises as a function of temperature than with a fixed cubic power. The same is found to be true with the second sound results of Wiarda et al. [12]. *

In fig. 11 the results of the extra attenuation of second sound in superfluid flow as observed by Wiarda and Kramers [10-12], are compared with the results from the present experiment. The values of F_{sn} from the second-sound research are computed from

$$F_{sn} = \frac{\rho_s \rho_n}{\rho} \frac{\omega_o}{Q_o} (y_o/y_m - 1)\, v_s .$$

ω_o is the angular frequency and Q_o the quality factor of the resonator without flow. y_o and y_m are the amplitudes of the second-sound signal, without and with a flow respectively. The relative velocities of the measuring points of the present study are corrected for a film contribution. Especially the values of F_{sn} from the wide capillary are very close to the values from the second-sound experiment. Unfortunately

Footnote *: The use of the value of v_s, at the previously [10] reported break, in the well-known critical velocity versus diameter graph of Van Alphen et al. [14] is no longer warranted.

there are no second-sound data available at higher velocities, because of the large attenuation at these velocities. Since the values of F_{sn} from our capillaries , having the same length, do not coincide, the mutual friction term F_{sn} probably depends on the diameter of the capillary.

2-4. *Connection between F_s and F_{sn}.* According to the theory of Hall and Vinen [2,15] the mutual friction force F_{sn} should be proportional to the total length of vortex line per unit volume L, multiplied by the relative velocity of the vortex lines and the excitations of the normal fluid,

$$F_{sn} = \alpha L (v_s - v_n), \tag{2.6}$$

with α a factor which does not depend on the velocities. If the pressure drop lF_s, as concluded from the present experiment, is connected with the vortices in the turbulent superfluid, this pressure drop might be put in the form,

$$F_s = \beta L, \tag{2.7}$$

with β an unspecified factor. These two forces will then be related by

$$F_s = \frac{\beta}{\alpha} \frac{F_{sn}}{(v_s - v_n)} . \tag{2.8}$$

In the figures 12 and 13 lF_s is plotted as a function of lF_{sn} divided

Fig. 12

The pressure drop lF_s, with a superfluid flow through the narrow capillary, as a function of the mutual friction term lF_{sn} divided by the relative velocity.

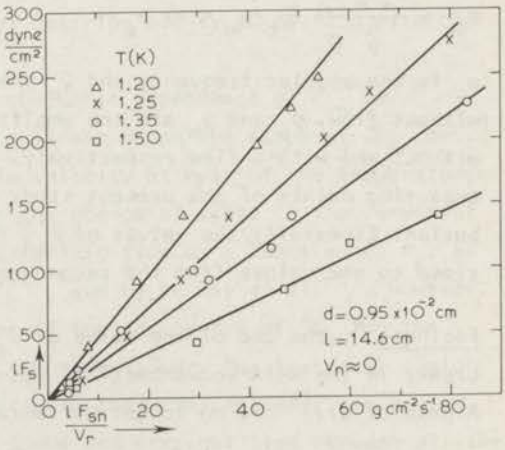

Fig. 13
The same quantities as in fig. 12
for the wide capillary.

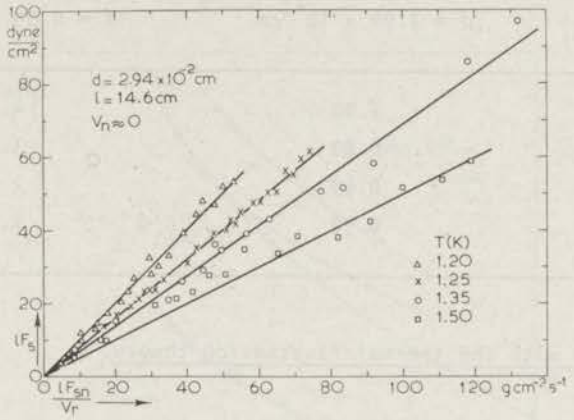

by v_r.

The relative velocities plotted are corrected for the film transfer. Though the relative magnitudes of F_s and F_{sn} in the two capillaries differ (see figs. 4a and 4b) the patterns shown in the figures 12 and 13 are similar. Therefore, we suggest that these graphs probably demonstrate that the equations (2.6) and (2.7) are generally valid in turbulent superfluid flow. Since the results, as given in the figures 12 and 13 can be represented by straight lines, β appears to be also independent of the velocities. The values of the quotient β/α, as calculated from the straight lines in the figs. 12 and 13, are given in table I.

If the pressure drop lF_s is caused by an interaction of the vortex lines with the wall, this interaction probably takes place via the normal fluid, since η_n seems to play a role in the determination of the pressure drop. Until now it is not clear in which way the present results can be related to the vortex line theories [2,15]. However, in our opinion, these results strongly suggest that the pressure drop lF_s and the mutual friction term lF_{sn} are both connected with the total length of vortex line per unit volume. In the following chapter such a relation will be shown to be present also at other velocity combinations.

Table I

Values of β/α in cm/s in the two capillaries.

T(K)	$d = 2.94 \times 10^{-2}$cm	$d = 0.95 \times 10^{-2}$cm
1.20	1.00	4.7
1.25	0.80	3.5
1.35	0.69	2.7
1.50	0.50	1.8

3. Comparison with the thermal-fluctuation theory.

The flow of superfluid helium in very small channels has been interpreted in terms of the thermal-fluctuctuation theory developed by Langer and Fisher [16]. Experiments explained in accordance with this theory have been performed by Clow and Reppy [17], Notarys [18], Liebenberg [19], Chester et al. [20], and Cannon et al. [21]. According to the theory of Langer and Fisher [16], Notarys [18] has shown that the chemical-potential drop $\rho\Delta\mu$ over a small channel should be proportional to the superfluid velocity v_s as

$$\rho\Delta\mu = A \exp(- B/v_s), \tag{3.1}$$

with A and B depending on the temperature, but not on v_s or $\rho\Delta\mu$. In order to verify whether such a dependence is also present in our experiment, a plot of lF_s and $\rho\Delta\mu$ on v_s^{-1} is made, as shown in fig. 14. The values of v_s are corrected for a film contribution. From this graph it is obvious that our measuring points do not obey eq. (3.1), since they can not be summarized with a straight line. Therefore, the thermal-fluctuation theory, though successful in very narrow channels, does not seem to account for the phenomena observed in our "wide" channels.

4. Conclusion.

In both capillaries the mutual friction force F_{sn} depends on the 2.75th

Fig. 14
The chemical-potential drop $\rho\Delta\mu$ and the pressure drop lF_s, as a function of v_s^{-1} at T = 1.25 K.

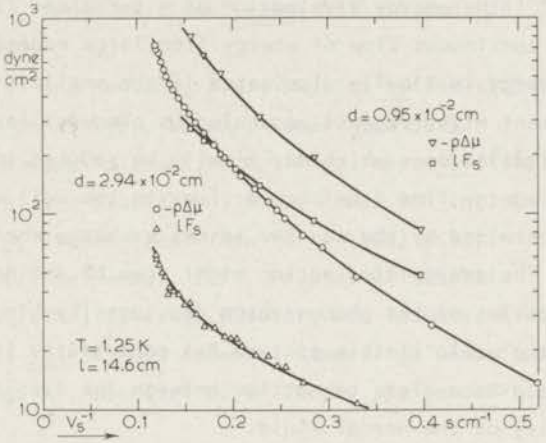

power of v_r at the lowest temperatures. This power rises slightly as a function of temperature, in accordance with the results from the second-sound experiment of Wiarda et al.[12].

With the narrow capillary lF_s, the pressure drop caused by the turbulently flowing superfluid, resembles the pressure drop observed with turbulent flow in classical hydrodynamics, at all temperatures studied. With the wide capillary lF_s is much smaller than in the narrow one but also seems to depend on the 1.75th power of v_s. However, these pressure drops are only 50 % of the pressure drops calculated from the empirical relation of Blasius.

Further, a connection has been found between the mutual friction force F_{sn} and the pressure drop lF_s. This connection suggests a common origin of the two forces. Probably both depend on the total length of vortex line per unit volume. The mutual friction force F_{sn} represents the interaction between the vortex lines and the normal fluid. This force represents a loss of momentum from the superfluid to the normal fluid. The pressure drop lF_s, suggesting an interaction of the vortex lines with the wall, describes the momentum loss from the superfluid to the wall. The force F_s

might be due to a momentum transfer to the wall by way of vortex lines attached to small irregularities of the wall. It is not clear, however, why η_n should play a role in this process. Another possibility might be a dissipation similar to the dissipation in ordinary fluids. In classical hydrodynamics [22] the energy dissipation of a turbulent flow can be described by a continuous flow of energy from large eddies to small ones. This flow of energy is finally dissipated in the smallest eddies. The present experiment might suggest an analogous process: larger vortices break up into smaller ones which may finally be reduced into rotons. This causes an energy flow from the vortices to the wall which may be essentially determined by the way the rotons exchange energy (or momentum) with the wall. The energy dissipation might then be dominated by the transport properties of the phonon-roton gas, possibly in a narrow boundary with the wall. If this picture has some truth, it is evident that there should be a close connection between the dissipative pressure and the viscosity of the normal fluid.

It will be clear that until our knowledge about turbulently flowing superfluid is substantially enlarged, these statements describing the possible mechanisms of F_{sn} and F_s, are only speculations.

References

1) Van der Heijden, G., De Voogt, W.J.P. and Kramers, H.C., Physica, to be published. (Commun. Kamerlingh Onnes Lab., Leiden No.392a). The first chapter of this thesis.
2) Vinen, W.F., Proc. Roy. Soc. A240(1957)114 and 128, 242(1957)493, 243(1958)400.
3) Gorter, C.J. and Mellink, J.H., Physica 15(1949)285 (Commun. Kamerlingh Onnes Lab., Leiden, Suppl. No. 98a).
4) Kidder, J.N. and Fairbank, W.M., Phys. Rev. 127(1962)987.
5) Kidder, J.N. and Blackstead, H.A., Proc. 9th int. Conf. on low Temp. Phys., LT 9, Plenum Press (New York, 1965) p.331.
6) Keller, W.E. and Hammel, E.F., Physics 2(1966)221.
7) Van Alphen, W.M., De Bruyn Ouboter, R., Taconis, K.W. and De Haas, W., Physica 40(1969)469 (Commun. Kamerlingh Onnes Lab., Leiden No.367a).
8) Schlichting, H., Boundary Layer Theory, Pergamon Press (London, 1955) p.401.
9) Staas, F.A., Taconis, K.W. and Van Alphen, W.M., Physica 27(1961)893 (Commun. Kamerlingh Onnes Lab., Leiden No. 328d).
10) Kramers, H.C., Superfluid Helium, ed. J.F. Allen, Academic Press (London and New York, 1966) p.199.
11) Wiarda, T.M., Thesis (Leiden, 1967).
12) Wiarda, T.M., Van der Heijden, G. and Kramers, H.C., to be published.
13) Le Ray, M., Bataille, J., François, M. and L'Huillier, D., Phys. Letters 31A(1970)249.
14) Van Alphen, W.M., Van Haasteren, G.J., De Bruyn Ouboter, R. and Taconis, K.W., Phys. Letters 20(1966)474.
15) Hall, H.E. and Vinen, W.F., Proc. Roy. Soc. A238(1956)204 and 215.
16) Langer, J.S. and Fisher, M.E., Phys. Rev. Letters 19(1967)560.
17) Clow, J.R. and Reppy, J.D., Phys. Rev. Letters 19(1967)289.
18) Notarys, H.A., Phys. Rev. Letters 22(1969)1240.
19) Liebenberg, D.H., Phys. Rev. Letters 26(1971)744.
20) Chester, M., Williams, D.R. and Motloch, C., Proc. 12th int. Conf. on low Temp. Physics, ed. E.Kanda, Academic Press of Japan (Tokyo, 1971) p.61.
21) Cannon, W.C., Chester, M. and Jones, B.K., to be published.
22) Landau, L.D. and Lifshitz, E.M., Fluid Mechanics, Pergamon Press (London, 1963) p. 119.

CHAPTER III

FLOW WITH v_n AND v_s UNEQUAL ZERO

Synopsis

Flowing liquid He II through a capillary is studied, for types of flow in which the velocities v_n and v_s, of the normal fluid and the superfluid respectively, can be varied independently. A survey of the measurements from all types of flow is given in diagrams of the (v_n, v_s) plane, in which curves of constant $\rho S \Delta T$, $\rho \Delta \mu$, and ΔP are given. These diagrams include curves for isothermal flow ($\Delta T = 0$), flow without a chemical-potential difference ($\Delta \mu = 0$), and isobaric flow ($\Delta P = 0$). The results indicate that the normal fluid is moving laminarly both in subcritical and supercritical flow. In supercritical flow apart of the mutual friction force F_{sn}, a frictional force F_s, connected with the superfluid, is observed. A general relation between the ratio F_{sn}/F_s and the relative velocity ($v_n - v_s$) is found. This relation might give an indication of a slip of the vortices relative to the superfluid.

1. Introduction

In a preceding chapter [1], referred to as I, the two versions a) and b) of the apparatus were described, in which the superfluid and normal component can be forced to flow simultaneously through a capillary, with independently adjustable velocities. A brief description of these devices can be given as follows. A closed circuit, partially filled with liquid helium, consists of a heat exchanger, and thermally insulated: the capillary, a superleak, an evaporator and a gaslink. Evaporation of liquid helium in the tube above the capillary and condensation of the helium gas in the heat exchanger results in a superfluid flow through the capillary. By superimposing this flow on a normal heat conduction flow, combinations of a superfluid and a normal fluid flow, either in the same or in opposite directions, can be produced. The quoted values of the velocities v_s and v_n, of the superfluid and normal fluid respectively, are averages over the capillary. Two stainless-steel capillaries of 2.94×10^{-2} cm and 0.95×10^{-2}

cm inner diameter, both 14.6 cm long, have been studied.

In order to investigate the forces acting on and between the two fluids, various types of flow have been studied. The chemical-potential drop $\rho\Delta\mu$ and the temperature difference ΔT over the capillary are determined as functions of the mean superfluid and normal fluid velocities (v_s, v_n). From these quantities the pressure drop ΔP over the capillary is calculated, using the integrated thermodynamic identity (neglecting velocity contributions), which for small values of ΔT and $\Delta\mu$, can be written as,

$$\Delta P = \rho S \Delta T + \rho \Delta\mu . \tag{1.1}$$

If $\rho\Delta\mu$ is not identically zero, the flow shall be called turbulent (supercritical).

In order to describe the experimental results for stationary flow in a capillary of length l, two quantities F_{sn} and F'_s are defined from the experimental results by:

$$0 = -\rho_s \frac{\Delta\mu}{l} - F_{sn} - F'_s , \tag{1.2}$$

and

$$0 = -\rho_n \frac{\Delta\mu}{l} - \rho S \frac{\Delta T}{l} + F_{sn} - F_n . \tag{1.3}$$

F_n is the normal viscous force. All the terms in these equations have the dimension of a force per unit volume. The fountain pressure $\rho S\Delta T$ and the normal fluid velocity v_n are calculated from the mean value of the entropy S and the temperature T in the capillary. The force F_{sn} corresponds with a mutual friction force as introduced by Gorter and Mellink [3], if the eqs. (1.2) and (1.3) are interpreted as the equations of motion for stationary flow.

From the eqs. (1.1) - (1.3), it follows that,

$$\Delta P = -lF_n - lF'_s . \tag{1.4}$$

The total pressure drop ΔP is composed of two contributions: a contribution lF_n from the moving normal fluid, and a contribution lF'_s connected with the superfluid flow. The first contribution, lF_n, corresponds with a pressure drop, together with a kinetic-energy correction, as observed in experiments with ordinary viscous fluids. From section I-3-3 it follows

that this latter correction is negligible in the experiments described in the present chapter. In the case of laminar flow of the normal fluid, $\mathcal{l}F_n$ is therefore found to be entirely determined by Poiseuille's law.

In chapter I, the pressure drop ΔP, obtained from the experiments with $v_s \simeq 0$, could be described completely with Poiseuille's law as well in sub- as in supercritical flow. In our opinion this indicates that F_s' is negligible in this case and that the normal fluid is flowing laminarly when $v_s \simeq 0$, even in supercritical flow.

In view of the experimental results of the present chapter, it will be shown that it is plausible to assume that the normal fluid also flows laminarly in types of flow with v_s unequal to zero. Consequently $\mathcal{l}F_n$ will be calculated from,

$$\Delta P_p(n) = -\, 8 \frac{\eta_n \mathcal{l}}{r^2} v_n = -\, \mathcal{l}F_n. \tag{1.5}$$

The second contribution to the total pressure drop ΔP, $\mathcal{l}F_s'$, equals the main term $\mathcal{l}F_s$ describing the "superfluid friction" in the capillary only, together with a kinetic-energy correction $\alpha \rho_s v_s^2$ originating from the exits of the capillary. In section I-3-3, α was estimated to be approximately equal to 1.0. Assuming that the normal fluid flows laminarly, the pressure drop corresponding with $\mathcal{l}F_s$ can be calculated from the experimental results by the relation:

$$-\, \mathcal{l}F_s = \Delta P + 1.0\ \rho_s v_s^2 + 8 \frac{\eta_n \mathcal{l}}{r^2} v_n. \tag{1.6}$$

In the second chapter [2] (referred to as II) the pressure drop corresponding with $\mathcal{l}F_s$, as derived from the experiments with turbulent superfluid flow, was discussed as describing a loss of momentum from the superfluid to the wall. This loss of momentum is probably connected with the generation and decay of vortex lines, or probably more correct deformed vortex rings, in the turbulent superfluid.

In the experiments reported in the present chapter, III, $\mathcal{l}F_s$ and $\mathcal{l}F_n$ both give an appreciable contribution to ΔP.

In order to obtain velocity combinations (v_n, v_s) in the regions of the velocity diagram between the lines $v_n = 0$ and $v_s = 0$, the following types of flow are studied:

a) flow with constant normal fluid velocity v_n and varying superfluid

velocity v_s;

b) flow with varying v_n and v_s, keeping their ratio v_n/v_s constant (in this manner e.g. flow without a relative velocity, $v_r = v_n - v_s = 0$, can be produced);

c) flow with a practically constant mass transport and varying v_n (at low temperatures, where $\rho_s >> \rho_n$, this nearly equals flow with constant v_s and varying v_n).

These types of runs are most conveniently realised with the present experimental set-up (see section I-2-2).

Every velocity combination (v_n, v_s) can be obtained with several types of flow. The cross-checks from different runs, even when carried out on different days, show good reproducibility, indicating that only the magnitudes and directions of the velocities are significant.

Both versions of the apparatus, a) and b), were described in detail in I. The flow through the wide capillary has been studied in both arrangements. Through the narrow one only a limited number of runs with v_n and v_s having the same sign are carried out. Since a changing level difference in the apparatus causes a correction to the velocities, in the narrow capillary very long times (longer than one hour) were found to be required for attaining stationary flow.

It should be noted that what is called the counterflow region in this chapter, covers the whole velocity region in which the superfluid and normal component move in opposite directions, contrary to the conventional use of the word "counterflow" which was restricted to no net mass flow ($\rho v = 0$) only.

Some preliminary results of the present experiments have already been published [4].

2. Experimental results

2-1. *Flow with v_n kept constant.* In fig. 1 the results for the wide capillary from two runs with v_n is constant are shown at $T = 1.35$ K. In fig. 1a the data for a pure superfluid flow are plotted as a function of the superfluid velocity v_s. In fig. 1b, the results for a run with v_n kept constant at 3.8 cm/s and varying v_s are plotted. The left side in both

Fig. 1

The fountain pressure $\rho S\Delta T$, the chemical-potential drop $\rho\Delta\mu$, and the pressure drop ΔP over the wide capillary as functions of v_s in two runs with v_n kept constant; 1a: $v_n = 0$; 1b: $v_n = 3.8$ cm/s.

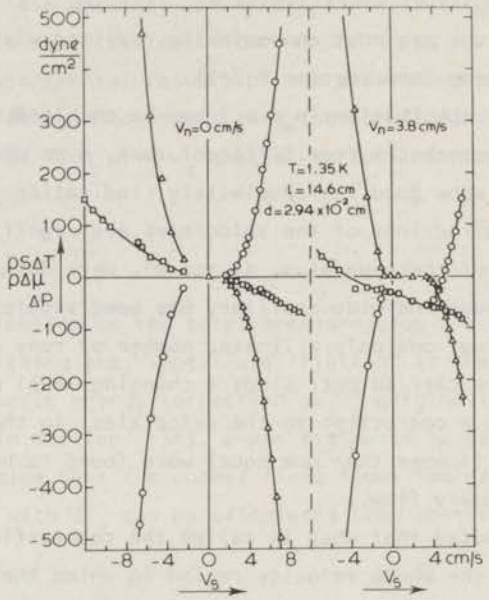

1a 1b

figures illustrates the results for the counterflow region.

In a possible subcritical region $\rho\Delta\mu$ is identically zero. Within the measuring accuracy the observed values of $\rho\Delta\mu$ are equal to zero in the region - 1.0 cm/s < v_s < 1.0 cm/s for pure superfluid flow, and in the region - 0.5 cm/s < v_s < 0.5 cm/s for flow with v_n = 3.8 cm/s. In these subcritical regions ΔP equals the pressure drop calculated from Poiseuille's law: lF_s remaining zero. In the supercritical parts, both lF_s and $\rho\Delta\mu$ are unequal to zero. Though in fig. 1b the subcritical region of the run with v_n = 3.8 cm/s seems to be more extended than mentioned above, $\rho\Delta\mu$ may be small, but is certainly not zero outside the quoted region. The limited extent of the subcritical region is more evident in the ΔP curve, where ΔP clearly deviates from $\Delta P_p(n)$ outside this region.

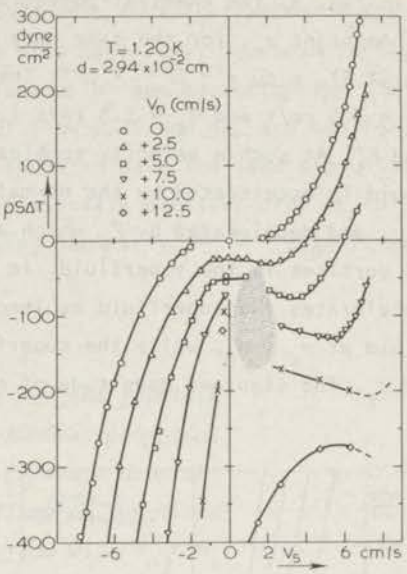

Fig. 2
The fountain pressure $\rho S\Delta T$ as a function of v_s for various runs with v_n kept constant. Shaded area: oscillatory region (l = 14.6 cm).

In the counterflow region of fig. 1b the line of ΔP rises if the magnitude of the velocity v_s is increased, indicating that $\mathcal{I}F_s$ and $\mathcal{I}F_n$ have opposite signs in the counterflow region. These two contributions to the total pressure drop may even balance each other: as is evident from fig. 1b at v_n = 3.8 cm/s and v_s = - 4.4 cm/s the flow is isobaric, i.e. a pressure gradient is absent.

On the right side of fig. 1b, at v_n = 3.8 cm/s and v_s = 5.0 cm/s, one point from an isothermal flow (ΔT = 0) is found. Contrary to the usual experiments [5-8] on isothermal flow, in which only the values of the mean velocity $v = (\rho_s v_s + \rho_n v_n)/\rho$ are known, from the present experiment the values of v_s and v_n, at ΔT = 0, can be obtained separately.

In fig. 2, the observed fountain pressure $\rho S\Delta T$ over the wide capillary, is shown as a function of the superfluid velocity v_s, for various values of the constant velocity of the normal fluid v_n (T = 1.20 K). Within the measuring accuracy $\rho S\Delta T$ equals the calculated Poiseuille pressure drop at $v_s \approx 0$. In the shaded area no stationary flow can be obtained, since ΔT oscillates between its value at v_s = 0 and a higher value. These oscillations will be discussed in section 3-3. In the counterflow region no oscillations have been observed.

In fig. 3, the chemical-potential drop $\rho\Delta\mu$ is shown as a function of v_s at constant v_n, for the same runs as reported in fig. 2. According to eq.(1.2), $\rho_s\Delta\mu = - \mathcal{L}F_{sn} - \mathcal{L}F'_s$. Therefore a point with $\rho\Delta\mu = 0$ (e.g. at $v_n = 7.5$ cm/s and $v_s = 5.3$ cm/s), represents a flow with balancing F_{sn} and F'_s. At such a velocity combination, with $v_n - v_s \simeq 2$ cm/s, the superfluid is accelerated by the normal fluid via the mutual friction force F_{sn}, and decelerated by F_s which apparently is connected with the creation of vortices in the superfluid. In general F_{sn}, in supercritical flow, decelerates the superfluid as long as $v_s > v_n$, and accelerates the superfluid at $v_s < v_n$, while the superfluid is decelerated by F_s at all values of v_s. The sign and magnitude of $\rho\Delta\mu$ depends on the magnitudes and signs

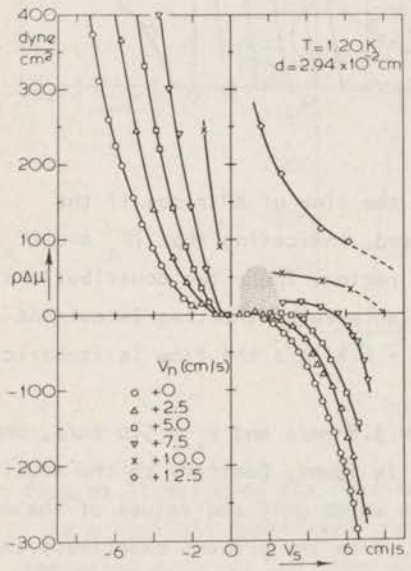

Fig. 3
The chemical-potential drop $\rho\Delta\mu$ as a function of v_s for various runs with v_n kept constant. Shaded area: oscillatory region (l = 14.6 cm).

of F_{sn} and F_s.

In the shaded part of fig. 3, the oscillations prevent the occurrence of a stationary flow, and $\rho\Delta\mu$ oscillates between zero and a positive value (see section 3-3).

No correction to v_s has been applied, to account for a possible film transfer (see section I-3-2), since the magnitude of the film correction is uncertain at values of $\rho\Delta\mu$ approximately equal to zero (see section 2-3).

2-2. *Flow with the ratio v_n/v_s kept constant.* An illustration of the results for a run with $v_n = v_s$ in the wide capillary, is shown in fig. 4 (T = 1.20 K). In this series, the values of v_s are corrected for the film transfer (0.2 cm/s). With this type of flow $\rho S\Delta T$ and $\rho\Delta\mu$ are smaller than the pressure drop ΔP, since they are found to have the same sign. The dotted line in fig. 4 represents the Poiseuille pressure drop $\Delta P_p(n)$ (eq.(1.5)). With the normal fluid moving laminarly $lF_n = -\Delta P_p(n)$. From

Fig. 4

Experimental points for the fountain pressure $\rho S\Delta T$, the chemical-potential drop $\rho\Delta\mu$, and the pressure drop ΔP over the wide capillary as functions of the velocity for flow with $v_n = v_s$.

The dotted line ($\Delta P_p(n)$) and the dashed line ($\Delta P_p(n) + \Delta P_B(s)$) are calculated (see text).

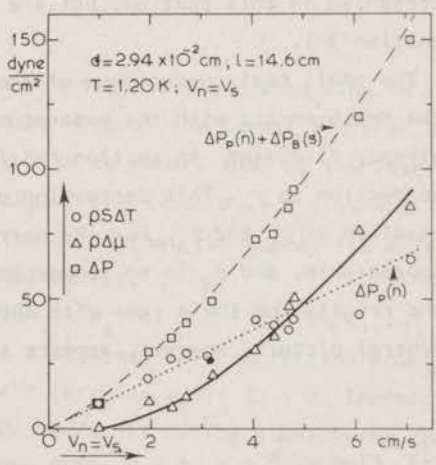

eq.(1.3) it follows that, at low temperatures where $\rho_n\Delta\mu \approx 0$, the fountain pressure $\rho S\Delta T$ nearly equals $-lF_n$, if $F_{sn} = 0$. As can be seen from fig. 4, the observed values of $\rho S\Delta T$ lie close to the $\Delta P_p(n)$ line. Therefore the same conclusion that was drawn in chapter I for flow with $v_s \approx 0$, that the normal fluid moves laminarly even in supercritical flow, applies for flow with $v_n = v_s$.

Turning now to the second part of ΔP one has to remember that in chapter

II (pure superfluid flow) the results for lF_s for the wide capillary appeared to be comparable with - 0.5 $\Delta P_B(s)$. This $\Delta P_B(s)$ was calculated from the modified Blasius rule for turbulent flow,

$$\Delta P_B(s) = - 0.158\, l \left[\frac{\rho^3 \eta_n v_s^7}{d^5} \right]^{\frac{1}{4}}. \qquad (2.1)$$

The results for lF_s, from runs with $v_n = v_s$ at temperatures ranging from 1.2 K to 1.5 K, however, are comparable with - $\Delta P_B(s)$. The dashed line in fig. 4 represents $\Delta P_P(n) + \Delta P_B(s)$, which corresponds well with the experimental data for ΔP (the kinetic-energy correction contributes only $\simeq 3$ % to ΔP). The increase of lF_s from $\simeq$ - 0.5 $\Delta P_B(s)$ at $v_n = 0$, to $\simeq$ - $\Delta P_B(s)$ at $v_n \simeq v_s$ will be described in the following section, where the results for types of flow with $\rho v \simeq$ constant will be given.

Since the results from measuring runs with v_n/v_s kept constant at 0.90 - 1.20 did not show any new aspects, these results will not be presented in this section, but are only given in the general surveys in section 3-1.

The small heat conductance of the superleak was measured only after the measurements with the apparatus type a) had been completed. As was already discussed in section I-3-1, the small heat leak leads to a correction to v_n. This correction disturbs the originally adjusted equality of v_s and v_n. For the narrow capillary this correction is appreciable, and v_n is no longer approximately equal to v_s. Therefore, the results for these runs with the narrow capillary are omitted. The general picture, however, appears to be the same in both capillaries.

2-3. *Flow with* $\rho_s v_s + \rho_n v_n$ *kept constant.*

2-3-1. *Experimental results for* ΔT *and* $\Delta\mu$. An illustration of the results for three series with $\rho v \simeq \rho_s v_{s,o} \simeq$ constant, is given in fig. 5 (T = 1.20 K, wide capillary). $v_{s,o}$ is the value of v_s at $v_n = 0$. At low temperatures (where $\rho_s \gg \rho_n$), the superfluid velocity v_s is almost constant with this type of flow: at T = 1.20 K, an increase of v_n of 16.5 cm/s corresponds to a decrease of v_s of 0.5 cm/s. In order to illustrate in detail the intersections of the lines of $\rho S \Delta T$ and $\rho \Delta\mu$ with the horizontal axis, only

Fig. 5
$\rho S\Delta T$ and $\rho\Delta\mu$ as functions of v_n for various runs with $\rho v \approx$ constant (l = 14.6 cm).

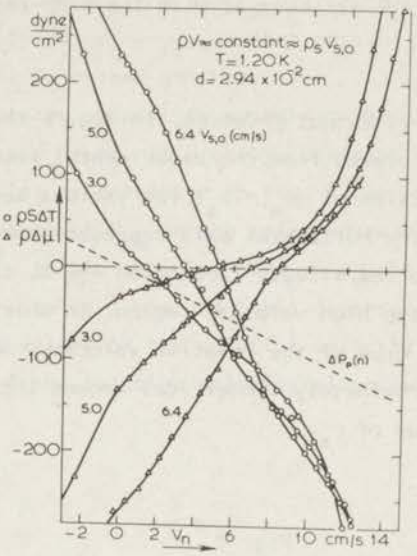

a part of these three series is plotted in fig. 5. The dashed line in fig. 5 represents the Poiseuille pressure drop of the normal fluid $\Delta P_p(n)$ as calculated from eq. (1.5). We should like to remark that at the intersections of the curves for $\rho S\Delta T$ with $\Delta P_p(n)$ one finds $v_s \approx v_n$, as was also found in section 2-2, and which indicates that the normal fluid is moving laminarly at these velocity combinations.

In section I-3-2 a possible correction to v_s, of 0.2 - 0.3 cm/s, to account for the film transfer has been discussed. This correction should decrease the calculated v_s if $\Delta\mu < 0$ and increase v_s if $\Delta\mu > 0$. Therefore, one might expect v_s to change with $\approx$ 0.5 cm/s, if during a measuring run the sign of $\Delta\mu$ changes. However, in fig. 5 there is no clear indication of such an abrupt change of v_s. It might be possible that the film transfer rate changes much more gradually through the point with $\Delta\mu = 0$. Because of this uncertainty about the magnitude of a possible film correction to v_s, no such a correction has been applied in this section.

The results from the measuring runs with $\rho v \approx$ constant at T = 1.35 K show the same pattern as at T = 1.20 K.

With the narrow capillary, only a few runs, all at different temperatures, have been studied. This limited number of data roughly shows the same

pattern as observed with the wide capillary.

2-3-2. *Mutual friction.* In fig. 6 the mutual friction term F_{sn}, as calculated from the experimental results with eq.(1.3), is plotted as a function of $(v_n - v_s)$ for various series with ρv = constant. The circles on the horizontal axis represent subcritical flow with $\rho v = 0$. As was reported already in section I-4-2, turbulent flow with $\rho v = 0$ was limited to the high velocity region, in which F_{sn} appeared to be proportional to the cube of the relative velocity. As can be seen in fig. 6, lF_{sn} is approximately symmetrical around the line $v_n - v_s = 0$, for a constant value of v_s.

Fig. 6

The mutual friction lF_{sn} as a function of $(v_n - v_s)$ for various runs with $\rho v \approx$ constant.

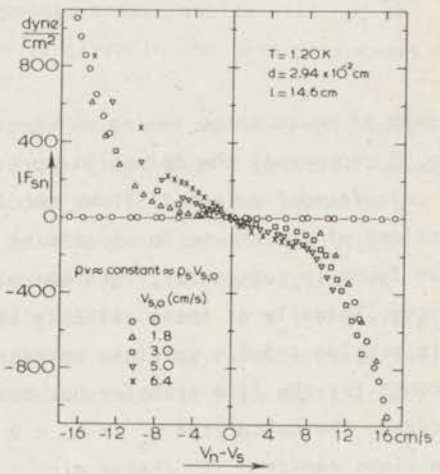

On the right side of fig. 6, a part of the measuring run with $v_{s,o}$ = 1.8 cm/s, is missing. At values of 2 cm/s < $(v_n - v_s)$ < 9 cm/s, oscillations prevented the determination of stationary values of $\rho S \Delta T$ and $\rho \Delta \mu$. At values of $v_{s,o}$ exceeding ≈ 2.5 cm/s no oscillations have been observed.

The results for F_{sn} shown in fig. 6, together with the results presented

in section 2-2, indicate that at $v_n = v_s$: $F_{sn} = 0$ and $F_n = -\Delta P_p(n)$. Bearing in mind that $\rho S \Delta T$ equals $\Delta P_p(n)$ at $v_n = v_s$, another possibility (e.g. with $F_{sn} \neq 0$ and $F_n \neq -\Delta P_p(n)$) is rather unlikely.

The functional dependence of F_{sn} on the velocities appears to be complicated. Since F_{sn} equals zero at $v_n = v_s$, it probably contains a factor $(v_s - v_n)^n$. However, the results as presented in fig. 6 can not be described by the simple cubic dependence of F_{sn} on the relative velocity as proposed by Gorter and Mellink [3]. In the vicinity of $v_n = v_s$ the relation of F_{sn} and $(v_n - v_s)$ appears to be linear. A cubic dependence of F_{sn} on $(v_n - v_s)$ is only found at values of the relative velocity larger than 8 cm/s. At high values of the relative velocity all curves probably coincide.

Fig. 7

The "superfluid friction" lF_s as a function of $(v_n - v_s)$ for various runs with $\rho v \approx$ constant (wide cap.) ($l = 14.6$ cm). For the significance of the error bars see text.

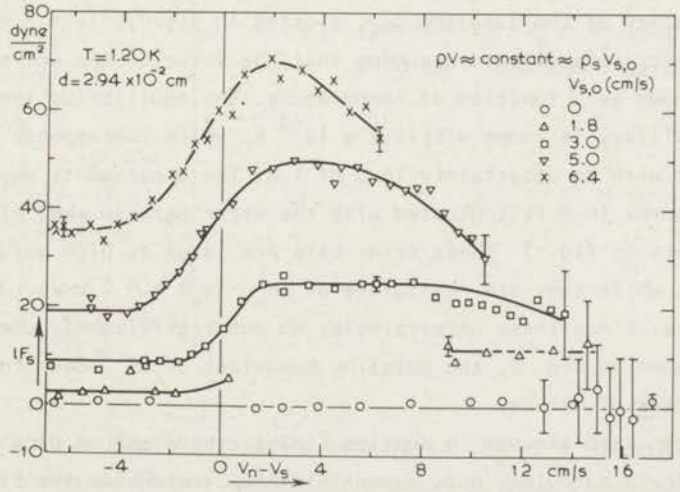

2-3-3. *The pressure drop corresponding with* $\mathcal{F}_s$. In fig. 7 the "superfluid friction" $\mathcal{F}_s$, for the wide capillary, is shown as a function of the relative velocity, for five series with ρv = constant. These data are obtained from the same runs as presented in the figs. 5 and 6. As was reported already in section I-4, $\mathcal{F}_s$ is negligible for both subcritical and supercritical flow with $v_s \simeq 0$. The "superfluid friction" $\mathcal{F}_s$, calculated from the results of runs with $v_{s,o} > 1.5$ cm/s, shows the following pattern. On the left side of fig. 7, $\mathcal{F}_s$ appears to depend on v_s only. In the vicinity of $v_n = v_s$, $\mathcal{F}_s$ increases till it reaches a maximum at $v_n - v_s \simeq 2$ cm/s. At these velocity combinations the chemical-potential drop $\rho\Delta\mu$ equals zero (see fig. 5). At values of $(v_n - v_s) >$ 2 cm/s, the results for $\mathcal{F}_s$ for runs for low values of v_s, differ from those at a high value of v_s. At low values of v_s, a new horizontal part indicates that $\mathcal{F}_s$ is again independent of v_n. At higher values of v_s, $\mathcal{F}_s$ decreases with increasing v_n. An extrapolation of the curves in fig. 7 to higher values of $(v_n - v_s)$, suggests that in the high velocity region all curves possibly coincide and finally tend to zero.

The few data we obtained at values of $(v_n - v_s) < -7$ cm/s are not plotted in fig. 7, since these data for $\mathcal{F}_s$ are very inaccurate. Probably $\mathcal{F}_s$ increases again at values of $(v_n - v_s) \simeq -12$ cm/s, however, the experimental results are not very conclusive.

The accuracy of the data for $\mathcal{F}_s$, plotted in fig. 7, is $\simeq 3$ dyne/cm^2. This accuracy is estimated assuming that the value of the entropy S is exactly known as a function of temperature. The equilibrium temperature of the capillary is known within 2×10^{-3} K, which corresponds in the experiment with an uncertainty in S of 1 %. The uncertainty due to this possible error in S is indicated with the error bars in some of the plotted data in fig. 7. These error bars are large at high values of $(v_n - v_s)$, while they are negligible at $(v_n - v_s) \simeq -2$ cm/s, where ΔT equals zero. Since these uncertainties do not significantly change the pattern shown in fig. 7, the puzzling behaviour of $\mathcal{F}_s$ seems to be a genuine trick of nature.

As was reported already in section II-2-2, the pressure drop corresponding with $\mathcal{F}_s$ for a turbulent pure superfluid flow, resembles the Blasius pressure drop observed in turbulent flow of ordinary liquids. A still stranger similarity with ordinary hydrodynamics seems to show up in the

type of flow expounded in the present section. Similar to the modified Blasius pressure drop $\Delta P_B(s)$ (see eq.(2.1)), a modified Poiseuille pressure drop $\Delta P_P(s)$ can be defined by:

$$\Delta P_P(s) = - 8 \frac{\eta_n l}{r^2} v_s . \qquad (2.2)$$

The values of lF_s at $v_n - v_s = 2$ cm/s, as calculated from the experiments, agree well with the values of $- \Delta P_P(s)$ and $- \Delta P_B(s)$, whichever is the greatest ($v_{s,o}$ is the value of v_s at $v_n = 0$):
at $v_{s,o} = 6.4$ cm/s: $- \Delta P_P(s) = 59$ dyne/cm^2 and $- \Delta P_B(s) = 70$ dyne/cm^2,
at $v_{s,o} = 5.0$ cm/s: $- \Delta P_P(s) = 46$ dyne/cm^2 and $- \Delta P_B(s) = 45$ dyne/cm^2,
at $v_{s,o} = 3.0$ cm/s: $- \Delta P_P(s) = 27$ dyne/cm^2 and $- \Delta P_B(s) = 18$ dyne/cm^2,
at $v_{s,o} = 1.8$ cm/s: $- \Delta P_P(s) = 13$ dyne/cm^2 and $- \Delta P_B(s) = 5$ dyne/cm^2.
This resembles very much to the results in ordinary hydrodynamics, in which one may find a laminar (Poiseuille) and a turbulent (Blasius) type of flow, while the stable flow corresponds with the largest pressure gradient of the two.

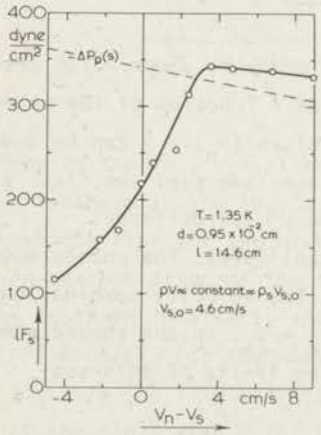

Fig. 8
The "superfluid friction" lF_s as a function of $(v_n - v_s)$ for a run with $\rho v \approx$ constant (narrow cap.).

As illustrated in fig. 8, the same pattern of lF_s as a function of $(v_n - v_s)$ is observed in the narrow capillary ($\rho\Delta\mu$ equals zero at $v_n - v_s = 2$ cm/s). In this run at $T = 1.35$ K, v_s decreases from 4.6 cm/s at $v_n = 0$ to 3.9 cm/s at $v_n = 12.6$ cm/s. This probably explains the slight

decrease of $\mathcal{I}F_s$ at values of $(v_n - v_s)$ exceeding 3.5 cm/s. The slope of $\mathcal{I}F_s$ at these values approximately equals the slope of the dashed line representing $-\Delta P_p(s)$ calculated from eq.(2.2).

Summarizing the results for $\mathcal{I}F_s$ for flow with ρv = constant for both capillaries:

1) $\mathcal{I}F_s$ increases in the vicinity of $v_n = v_s$ with increasing v_n;
2) $\mathcal{I}F_s$ no longer increases at $v_n - v_s \approx 2$ cm/s, where $\Delta\mu = 0$;
3) at low values of $v_{s,o}$, where $\Delta P_B(s) < \Delta P_p(s)$, $\mathcal{I}F_s$ levels off at a value that corresponds with a modified Poiseuille law (eq.(2.2));
4) at high values of $v_{s,o}$, where $\Delta P_p(s) < \Delta P_B(s)$, $\mathcal{I}F_s$ reaches a maximum value that corresponds with a modified Blasius rule (eq.(2.1));
5) at values of $v_{s,o}$ larger than 3 cm/s, $\mathcal{I}F_s$ is found to decrease at the highest values of $(v_n - v_s)$ that have been observed. Possibly all curves of $\mathcal{I}F_s$ coincide at still higher values of $(v_n - v_s)$.

Until now this behaviour of $\mathcal{I}F_s$, and its possibly unexpected resemblance with the results for an ordinary viscous fluid, are not yet understood.

3. Survey of the results from all types of flow

3-1. *The temperature, chemical-potential and pressure drops.* From the intersections of the curves of $\rho S\Delta T$ or $\rho\Delta\mu$, as a function of the relevant velocity, with the abscisses, the velocity values (v_n, v_s) can be deduced at which flow with $\Delta T = 0$ or $\Delta\mu = 0$ takes place (see e.g. the figs. 2,3, and 5). These values of the velocities v_n and v_s for different temperatures are collected in fig. 9 (wide capillary). The points above the line $v_n = v_s$, represent isothermal flow. The velocity combinations for which $\Delta\mu = 0$, are those below the line $v_n = v_s$. In the shaded area, $\Delta\mu$ is identically zero (subcritical flow). The limits of this subcritical region are not very well defined.

As can be concluded from eq.(1.2), $\Delta\mu$ equals zero if F_{sn} and F'_s balance each other. At low temperatures, where ρ_n is small, the condition for isothermal flow appears from eq.(1.3) to be a balancing of F_{sn} and F_n.

For the wide capillary, the curves of (v_n, v_s) at which isothermal flow or flow with $\Delta\mu = 0$ has been observed, are found to be temperature independent in the velocity region studied. For both capillaries the

Fig. 9

Isothermal flow (upper curve) and flow without a chemical-potential drop (lower curve) in the velocity plane (v_n, v_s). In the shaded region $\Delta\mu$ is identically zero (l = 14.6 cm).

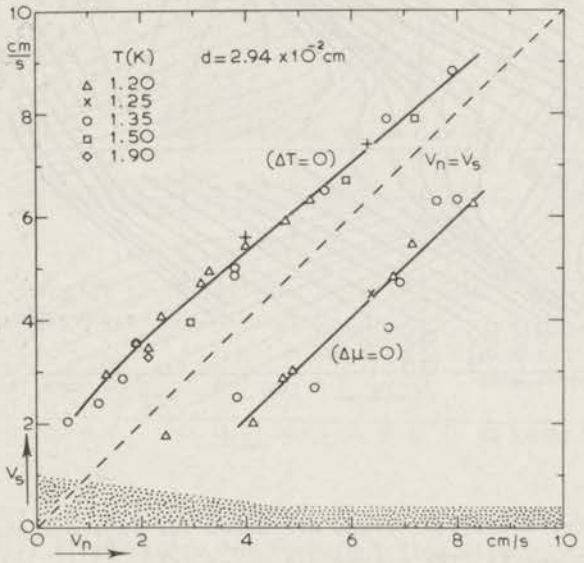

lines in the (v_n, v_s) plane with $\Delta\mu$ = 0 coincide. For the narrow capillary the isotherm in the (v_n, v_s) plane was found to lie approximately 2 cm/s above the line for the wide capillary shown in fig. 9.

An extrapolation of the data for ΔT = 0 shown in fig. 9, suggests that the isotherm intersects the axis v_n = 0 at the critical velocity $v_{s,c}$ (≈ 1.0 cm/s). For the narrow capillary $v_{s,c}$ can be estimated to be ≈ 3.0 cm/s (no film corrections have been applied).

If one plots grad P for the isothermal measuring points as a function of the mean velocity $v = (\rho_s v_s + \rho_n v_n)/\rho$, the curves show a similar behaviour as those found in other experiments on isothermal flow (see e.g. Atkins [5]).

In the figures 10 and 11 curves of constant $\rho S\Delta T$ and $\rho\Delta\mu$ respectively, are drawn in the (v_n, v_s) plane (T = 1.20 K). Because of the symmetry

Fig. 10

Lines of constant $\rho S\Delta T$ in the (v_n, v_s) plane. Dotted area: oscillatory region (l = 14.6 cm).

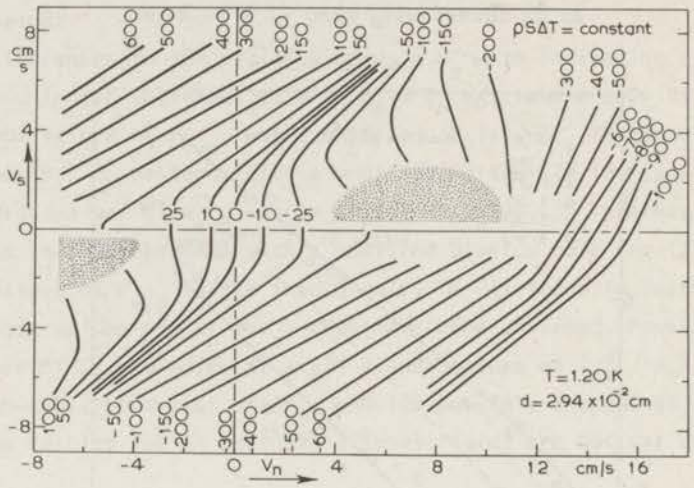

of the capillary, identical curves are drawn for (v_n, v_s) and (- v_n, - v_s) in the figs. 10 and 11. The quoted values of $\rho S\Delta T$ and $\rho\Delta\mu$ in the figs. 10 and 11 are in dyne/cm^2.

In order to illustrate the pattern in the vicinity of the curves with $\Delta T = 0$ or $\Delta\mu = 0$, curves for 10, 25, 50, and 150 dyne/cm^2 are given in addition to the curves for multiple values of 100 dyne/cm^2.

In the lightly dotted bulb in both figs. oscillations prevent the observation of stationary flow, while the shaded area around the absciss in fig. 11 indicates the velocity region at which subcritical flow takes place. In this subcritical region $\rho S\Delta T$ equals the Poiseuille pressure drop caused by the moving normal fluid, as is demonstrated by the intersections of the curves of $\rho S\Delta T$ = 10, 25, and 50 dyne/cm^2 with the axis $v_s = 0$.

At values of $v_n > 13$ cm/s, a flow with $v_s \approx 0$ may be subcritical as well as supercritical (see section I-4). For reasons of simplicity only the results for turbulent flow at these high values of v_n are used in the

Fig. 11

Lines of constant $\rho\Delta\mu$ in the (v_n, v_s) plane. Dotted bulb: oscillatory region. In the shaded area $\Delta\mu$ is identically zero (l = 14.6 cm).

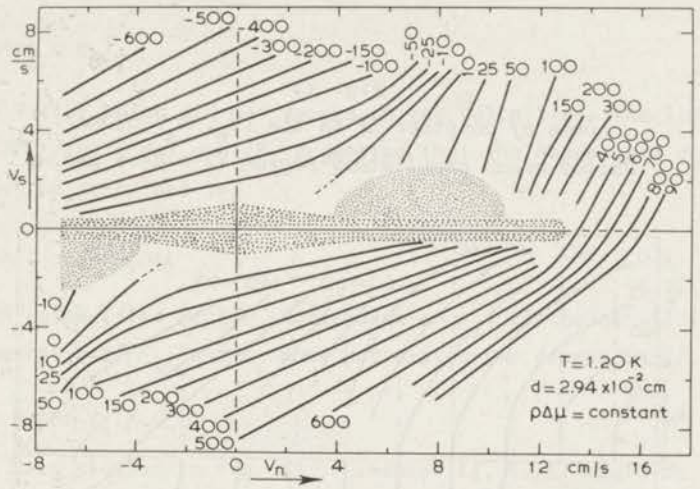

figs. 10 and 11. The results for turbulent flow with $v_s \approx 0$ fit into the pattern given by flow with $v_s \neq 0$.

At values of v_n < 13 cm/s, the curves for $\rho\Delta\mu$ = 400, 300 etc. are interrupted since no turbulent flow has been observed in the region around the line v_s = 0. These interruptions in fig. 11 are more extensive than the subcritical region, since, unfortunately, no measuring runs slightly above and below the subcritical region have been carried out, and an extrapolation of the curves to the limits of the subcritical region is doubtful. These remarks also apply to the interrupted curves in fig. 10.

The smoothed curves in the (v_n, v_s) velocity diagram, for constant values of the uncorrected pressure drop $\Delta P = \rho S \Delta T + \rho\Delta\mu$, are shown in fig. 12 ($T$ = 1.20 K). Again the dotted area indicates the oscillatory region. The vertical dashed lines indicate the pattern that would have been observed if only $\Delta P_p(n)$, the Poiseuille pressure drop of the normal fluid, had been present i.e. if $\mathcal{L}F_s'$ had been zero. At $v_s \approx 0$, $\mathcal{L}F_s'$ is negligible and $\rho S \Delta T = \Delta P_p(n)$ (see section I-4).

A remarkable result, illustrated in fig. 12, is the possibility of isobaric flow. In our opinion this is the first experiment in which the existence of flow without a pressure drop is observed!
This phenomenon is clearly connected with the peculiar two-fluid composition of liquid He II.

Fig. 12

Lines of constant ΔP in the (v_n, v_s) plane.
Dotted area: oscillatory region (l = 14.6 cm).

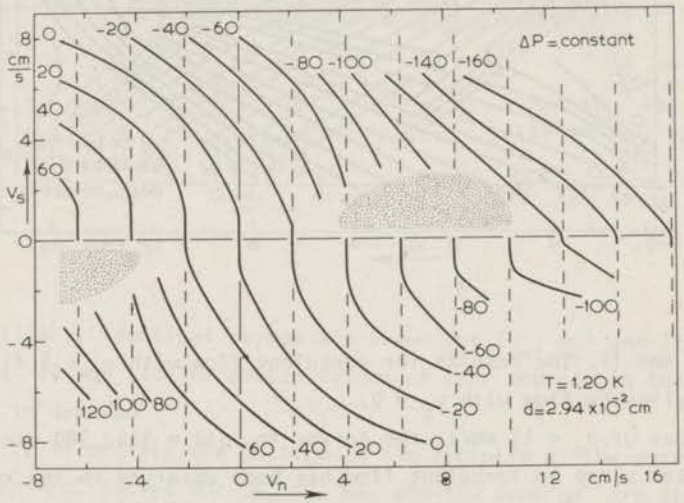

Contrary to the results of other experiments in the counterflow region [9,10] (see section I-4), in the present study the directions of the forces F_s and F_n, are found to be exclusively opposite to the direction of the velocity of the corresponding fluid, since both forces extract momentum from the flow of the corresponding components. Therefore the pressure drops in the counterflow region, concluded from the present experiment, are <u>smaller</u> than the value of $\Delta P_p(n)$ caused by the moving normal fluid alone.

At T = 1.35 K, roughly the same pattern as shown in the figs. 10-12 for T = 1.20 K, has been observed. With the narrow capillary no systematic investigations, at a fixed temperature, have been performed.

3-2. *Connection between F_{sn} and F_s.* In section II-2-4, a linear relation between $\mathcal{l}F_s$ and $\mathcal{l}F_{sn}/(v_s - v_n)$, for a pure superfluid flow, was reported. This relation suggested that both F_{sn} and F_s are proportional to L, the total length of vortex line per unit volume. According to the theory of Hall and Vinen [11,12], the mutual friction force F_{sn} should be proportional to L multiplied by $(v_s - v_n)$,

$$F_{sn} = \alpha L(v_s - v_n), \tag{3.1}$$

with α a factor which did not depend on the velocities. The linear relation between $\mathcal{l}F_{sn}/(v_s - v_n)$ and $\mathcal{l}F_s$ suggested that the dependence of F_s on L could best be described by,

$$F_s = \beta L , \tag{3.2}$$

with β an unspecified factor independent of v_s. If the eqs.(3.1) and (3.2) hold, the ratio of F_{sn} and F_s does not explicitly depend on L:

$$F_{sn}/F_s = (\alpha/\beta)(v_s - v_n). \tag{3.3}$$

From the data plotted in fig. 13 of chapter II, (α/β) could be deduced.

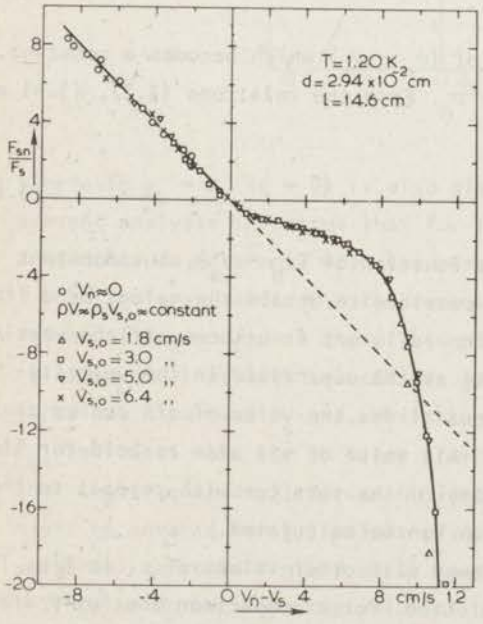

Fig. 13
Data for F_{sn}/F_s as a function of $(v_n - v_s)$ from various measuring runs.

As can be seen from fig. 13 of the present chapter, the ratio F_{sn}/F_s for other types of flow still only depends on $(v_n - v_s)$, but shows a more complicated behaviour (the plotted data are for runs with v_n and v_s having the same sign). The behaviour of the ratio F_{sn}/F_s as a function of $(v_n - v_s)$ in the velocity region where $v_n > v_s$, indicates that one or more of the simple assumptions made in chapter II do not hold for all velocity combinations. Until now no unambiguous understanding of the results shown in fig. 13 has been reached. However, a rather speculative explanation might be the following.

Originally Hall and Vinen [11] suggested that F_{sn} should depend on L as,

$$F_{sn} = \gamma L(v_L - v_n), \tag{3.4}$$

in which v_L is the vortex line velocity and γ is independent of the velocities. Using the unproved assumption that v_L and v_s are equal, Vinen [12] obtained relation (3.1). The possibility that $(v_L - v_s)$ is non-zero will be considered in the following. We still assume eq.(3.2) holding for all types of flow. The ratio F_{sn}/F_s, as obtained from the present experiments, can still be described by

$$F_{sn}/F_s = \psi\ (v_s - v_n), \tag{3.5}$$

with now ψ in general a function of $(v_n - v_s)$ which becomes a constant, however, in the region where $v_s > v_n$. From the relations (3.2), (3.4) and (3.5) it follows that,

$$v_L - v_n = \varepsilon\ (v_s - v_n), \tag{3.6}$$

with $\varepsilon = (\psi\beta/\gamma)$ also in general a function of $(v_n - v_s)$, but constant for $v_s > v_n$. It is, however, not possible to obtain the values of ε from the experimental results, since the ratio γ/β is unknown. If the vortices should move with the same velocity as the superfluid in the velocity region where $v_s > v_n$, ε should equal 1 and the value of γ/β can be derived immediately. Of one then assumes this value of γ/β also to hold for flow with $v_n > v_s$, the relative velocity of the vortices with respect to the superfluid for these types of flow can be calculated.

The same procedure can be followed with other values of ε. In fig. 14 curves for $\varepsilon = \frac{1}{2}$ and $\varepsilon = 1$ are plotted. For a comparison the fully drawn

Fig. 14

The calculated velocities of the vortices relative to the superfluid as a function of $(v_n - v_s)$*, for constant values of* γ/β*, adapted by means of chosen values of* ε *in the velocity region where* $v_s > v_n$*. For details see text.*

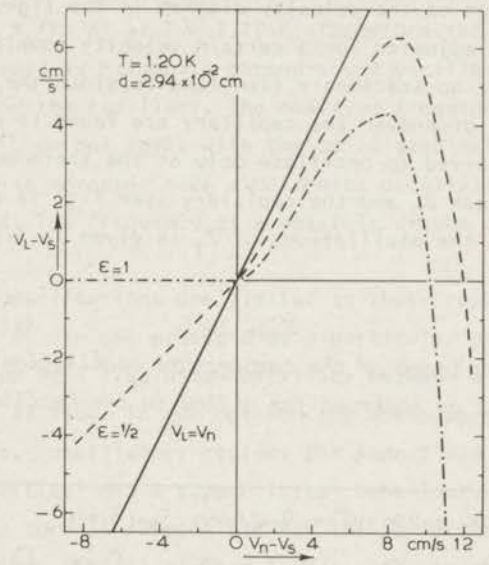

line with $v_L = v_n$ ($\varepsilon = 0$) is also given. As can be seen from fig. 14, the present analysis indicates that for flow with $v_n > v_s$, the vortices show a tendency to move more with the normal fluid than with the superfluid.

Both for $\varepsilon = \frac{1}{2}$ and $\varepsilon = 1$ the curves for $v_L - v_s$ sharply decrease for values of $(v_n - v_s) > 8$ cm/s. This might be due to an invalidity of relation (3.2) at high velocities. As was mentioned earlier, $F_s \simeq 0$ for turbulent flow with $v_s \simeq 0$, while the simultaneously non-zero value of F_{sn} indicates that yet vortices are present. Since L can not be zero in that case, relation (3.2) can no longer be valid. Therefore relation (3.2) might be invalid for all values of $(v_n - v_s)$ exceeding 8 cm/s, though the universal curve in fig. 13 still seems to persist.

Since we do not know the value of ε, the magnitude of $(v_L - v_s)$ is

uncertain. Moreover, the values for $(v_n - v_s)$ as plotted in the figs. 13 and 14 are mean values, while the velocities in eq.(3.4) are not averaged! However, in our opinion the results for F_{sn}/F_s suggest that a slip of the vortices relative to the superfluid might play a significant role.

3-3. *Oscillations.* In the wide capillary oscillations have been observed in the dotted region of the velocity diagram in the figs.10, 11, and 12. If the heaters are adjusted for a certain velocity combination (v_n, v_s) inside this region, no stationary flow results, since the temperature and chemical-potential drop over the capillary are found to oscillate. The temperature is observed to oscillate only at the thermometer T_2 mounted between the superleak S_2 and the capillary (see fig. 1a of chapter I). An illustration of the oscillations of T_2 is given in fig. 15.

Fig. 15

A recorder trace of the temperature oscillation of the thermometer T_2, as observed for a flow in the oscillatory region.

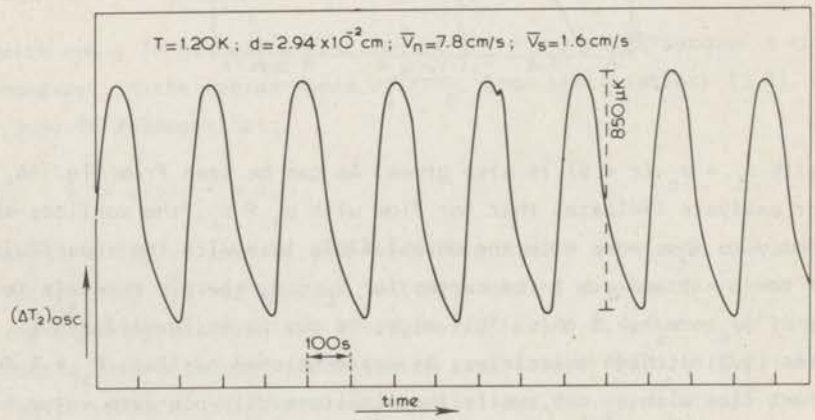

These oscillations show an exactly recurring pattern during more than one hour. Moreover, the same pattern is observed with runs on different days. No damping of the oscillations has been found. The oscillation of the temperature at T_2 induces a correction to v_n, since the helium in the

vicinity of T_2 warms up or cools down, resulting in a smaller or larger v_n through the capillary respectively. The oscillation of $\rho\Delta\mu$ is obtained from the oscillation of the helium level h_3 (see fig. 1a of chapter I), h_4 being approximately constant. Since the temperature drop $T_1 - T_3$ is constant, the level h_1 also oscillates, causing a correction to the calculated v_s. From the observed oscillations of T and h, the oscillations of v_n and v_s are calculated to be reverse and of the same order of magnitude. This is contrary to a second-sound oscillation, where $v_n >> v_s$ since $\rho_s >> \rho_n$ at T = 1.20 K. Therefore the observed oscillations cannot be regarded as Helmholtz second-sound oscillations between the volume at T_2 and the capillary. The observed frequencies, ranging from 0.05 - 0.01 s^{-1}, do not agree with the calculated Helmholtz frequency of 1.5 s^{-1}, while moreover such a Helmholtz oscillation should be very strongly damped. The frequency of a possible U-tube oscillation should be 0.15 s^{-1}.

The observed oscillations are similar to those reported in ordinary hydrodynamics [13]. In the presence of a particular pressure drop over a tube, the flow of a liquid may oscillate between a laminar and a turbulent type of flow. In our opinion the analogue of this phenomenon is present in our oscillatory region: the superfluid flow oscillates between a subcritical and a supercritical behaviour, producing a varying ΔT which in its turn is responsible for the variation of v_n.

The oscillations are illustrated in fig. 16a. In this figure the extreme values of $\rho\Delta\mu$ are shown as a function of the mean value of v_n for a run with $\rho v \approx$ constant. The values of $\rho\Delta\mu$ are calculated from the maximum and minimum heights of h_3 and h_4, which however cannot be determined very accurately. At values of v_n exceeding 10.5 cm/s stationary flow is present, and the results for this stationary flow fit with the maxima of $\rho\Delta\mu$ for the oscillating measuring points.

In fig. 16b the period ν^{-1} of the oscillations is plotted as a function of the mean value of v_n. These periods are deduced from the recorder traces for ΔT and appear to be roughly proportional to the amplitudes of the oscillations of $\rho\Delta\mu$ (compare fig. 16a).

The frequency and the magnitude of the oscillations only depend on the mean value of v_n and not on the mean value of v_s.

In the narrow capillary, oscillations have been observed in a run with

Fig. 16b

The period of the oscillations shown in fig. 16a as a function of the mean value of v_n.

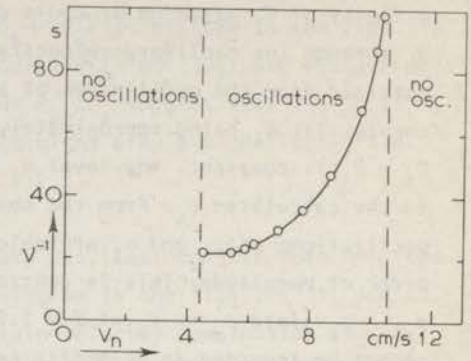

Fig. 16a

Values of $\rho\Delta\mu$ as a function of the mean value of v_n, for a series with $\rho v \approx$ constant in the oscillatory region. The dashed lines connect the maximum and minimum values at the oscillating points.

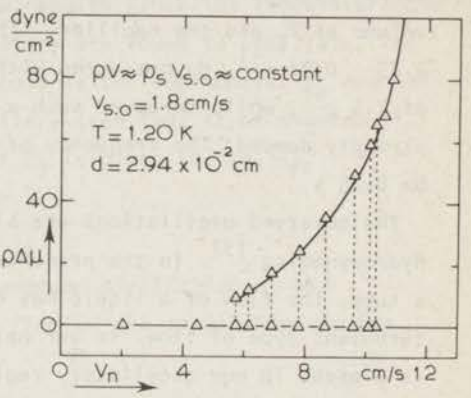

$\rho v \simeq \rho_s \times 1.0$, for values of v_n exceeding 6 cm/s. Because of the very large periods, ranging from 110 s at v_n = 6.6 cm/s up to 600 s at v_n = 11 cm/s, no higher values of v_n have been studied.

Concluding: in the oscillatory region of the velocity diagram for the wide capillary, the superfluid flow probably oscillates between a subcritical flow with $\rho\Delta\mu = 0$ and a supercritical flow with $\rho\Delta\mu > 0$. The maximum values of $\rho\Delta\mu$ correspond well with the data which can be deduced from an extrapolation of the curves for constant $\rho\Delta\mu$ in fig. 11.

4. NRS FLOW

If the present apparatus is completely filled with liquid helium, a type of flow can be produced that was studied first by Staas, Taconis and Van Alphen [14]. In section 2-5 of chapter I, we called this type of flow NRS flow. In this type of flow only the velocity of the normal fluid is adjustable, while a possible superfluid flow is not externally

restricted (Non Restricted Superfluid flow). As was explained in chapter 1, the chemical-potential drop always equals zero in this type of flow, and $\rho S \Delta T = \Delta P$. From fig. 11 of the present chapter it is clear that at a certain value of v_n there are two possibilities for v_s at which the superfluid flow may adjust itself, keeping in mind the condition that $\rho\Delta\mu$ remains zero. On the one hand v_s may be approximately zero. In this case an NRS flow is subcritical and only the laminarly flowing normal fluid contributes to ΔP. On the other hand v_s may lie on the solitary line with $\rho\Delta\mu = 0$ (fig. 11), at which F_{sn} and F_s' balance each other. In that case an NRS flow is composed of a superposition of a laminar normal fluid flow and a turbulent superfluid flow.

These two possibilities are illustrated in fig. 17: the measuring points on the lowest line (with a slope of 1.0) represent subcritical flow, the measuring points lying above this line supercritical flow. During a measuring run with NRS flow hysteresis may take place: subcritical flow changes abruptly into supercritical flow. If turbulence is present, a following decrease of v_n down to approximately 2 cm/s is required in order to obtain again subcritical flow.

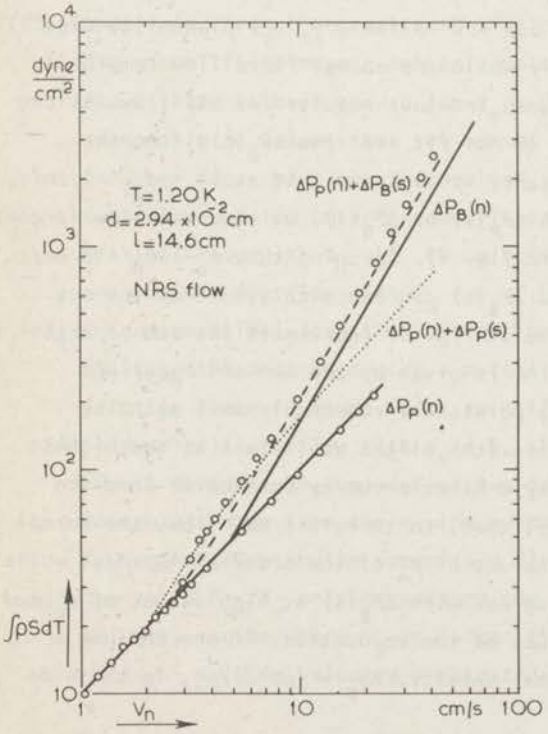

Fig. 17
The fountain pressure as a function of v_n, observed for NRS flow. The lines are calculated (fully drawn lines according to Staas et al.).

With turbulent NRS flow ($v_s \simeq v_n - 2$ cm/s, see fig. 11), the interaction of the normal fluid with the vortices causes a drag on the superfluid. If v_n is small ($\simeq 2$ cm/s), the vortices probably disappear and a careful raising of v_n results again in a subcritical flow.

As was mentioned already NRS flow was studied first by Staas, Taconis and Van Alphen [14]. According to these authors their results could be represented by two relations (the notation differs from that in ref. 14):

$$\Delta P_P(n) = - 32 \frac{\eta_n l}{d^2} v_n \ , \tag{4.1}$$

$$\text{and } \Delta P_B(n) = - 0.158\, l \left(\frac{\rho^3 \eta_n v_n^7}{d^5} \right)^{\frac{1}{4}} . \tag{4.2}$$

The eqs. (4.1) and (4.2) describe their subcritical and supercritical results respectively. In order to interpret their results on supercritical flow, these authors assume the entire liquid to be turbulent. In fig. 17 the solid lines $\Delta P_P(n)$ and $\Delta P_B(n)$ are calculated from the eqs. (4.1) and (4.2).

From our experiments with a partly filled apparatus, the conclusion can be drawn that on the line with $\rho\Delta\mu = 0$ in the (v_n, v_s) plane (see fig. 11), the superfluid flows turbulently while the normal fluid flow remains laminar. The same can be concluded from our results for NRS flow. As can be seen in fig. 17 our results do not fit the line $\Delta P_B(n)$. From the results of flow with $\rho v \simeq$ constant, it is known that at $v_n - v_s \simeq 2$ cm/s, where $\Delta\mu = 0$, $- lF_s$ agrees with $\Delta P_P(s)$ or $\Delta P_B(s)$, whichever is the largest. The same behaviour is present in fig. 17. Assuming that $v_s \simeq v_n - 2$ cm/s at all values of v_n, $\Delta P_P(s)$ and $\Delta P_B(s)$ can be calculated from the eqs. (2.2) and (2.1). The dotted line in fig. 17 represents the sum of $\Delta P_P(n)$ and $\Delta P_P(s)$, while the dashed line is given by the sum of $\Delta P_P(n)$ and $\Delta P_B(s)$. The turbulent measuring points fit reasonably well with the largest calculated pressure drops (the slight deviations at the highest values of v_n can be explained by a kinetic-energy correction from the superfluid). The results suggest that, in turbulent NRS flow, the normal fluid flows laminarly even at values of v_n of the order of 40 cm/s, while the "superfluid friction" lF_s agrees with $\Delta P_B(s)$ at high values of v_n and v_s, and with $\Delta P_P(s)$ at low values of the velocities. If one defines a Reynoldsnumber Re_v with the total density, $Re_v = (\rho v_n d)/\eta_n$, in the wide

capillary a velocity of 40 cm/s at T = 1.20 K corresponds with a value of Re_v of 10^4.

The reason for the difference between the results of Staas et al. [14] and the results from the present experiment is unknown. However, the results of Staas at low temperatures, with a capillary of $d = 0.82 \times 10^{-2}$ cm (fig. 6 of ref. 14), also indicate a deviation from eq.(4.2) at low values of Re_v. This deviation strongly resembles our results illustrated in fig. 17, suggesting that with their narrowest capillary deviations of relation (4.2), similar to our deviations, were present.

5. Conclusion

In the presented experiments the fountain pressure $\rho S \Delta T$, the chemical-potential drop $\rho \Delta \mu$, and the pressure drop ΔP over a capillary have been determined as functions of the velocity pair (v_n, v_s), for various types of flow through a capillary. Only a limited range of velocities have been studied, since in general v_s and v_n did not exceed 10 cm/s and 20 cm/s respectively. From the results the following conclusions can be drawn.

1) The normal fluid moves laminarly both in subcritical and supercritical flow. This has been proved for $v_s \simeq 0$ and $v_n = v_s$. Therefore it is reasonable to assume that the normal fluid is also flowing laminarly in other types of flow. The maximum values of v_n studied in the wide capillary are: 50 cm/s for subcritical NRS flow, 22 cm/s for subcritical flow with $v_s \simeq 0$, 16 cm/s for supercritical flow with $v_s \simeq 0$, and 10 cm/s for flow with $v_n = v_s$.
2) In supercritical flow the interaction of the superfluid and the normal fluid can be described with a mutual friction force F_{sn}. This mutual friction force is found to be zero if $v_n - v_s = 0$.
3) In supercritical flow with $v_s \neq 0$, the pressure drop over the capillary, ΔP, is found to be composed of two additional contributions: a Poiseuille drop from the moving normal fluid and a "superfluid friction" $\mathcal{L}F_s$ connected with the superfluid flow.
4) The ratio F_{sn}/F_s only depends on the relative velocity $(v_n - v_s)$. In the velocity region where v_s is larger than v_n, F_{sn}/F_s is a linear function of $(v_n - v_s)$. At velocity combinations with v_n larger than v_s a more

complicated dependence of F_{sn}/F_s on $(v_n - v_s)$ appears.

5) Three special lines in the (v_n, v_s) plane have to be noted.

a) On a line slightly above the line $v_n = v_s$, the flow is observed to be isothermal ($\Delta T = 0$). At these velocity combinations the two friction forces acting on the normal fluid, i.e. the mutual friction force F_{sn} and the viscous force F_n, balance each other practically. The position of this line depends on the diameter but not on the temperature.

b) On a line $(v_n - v_s) \approx 2$ cm/s, flow without a chemical-potential drop is observed. At these velocity combinations the two forces acting on the superfluid, F_{sn} and F_s, are balancing. The position of this line does not depend on the diameter or the temperature.

c) In the counterflow region, a line on which $\Delta P = 0$ is found. At these velocity combinations the friction forces F_n and F_s, connected with the corresponding fluids, balance each other, giving rise to an isobaric flow.

Apart from these conclusions the following remarks may be made.

The lines in the (v_n, v_s) plane on which $\Delta T = 0$ or $\Delta\mu = 0$, are found to be temperature independent for $1.20\ \mathrm{K} \leqslant T \leqslant 1.50\ \mathrm{K}$. This result seems to be surprising, since the mutual friction force F_{sn}, at a fixed value of $(v_n - v_s)$, is usually observed to be highly temperature dependent [3,11,12], while F_n only weakly depends on the temperature. However, $\Delta T = 0$ for small values of $(v_n - v_s)$ only, and the usual experiments on F_{sn} were carried out at large values of $(v_n - v_s)$.

The "superfluid friction" $\mathcal{I}F_s$ apparently describes that part of the total loss of momentum of the superfluid, $(\mathcal{I}F_{sn} + \mathcal{I}F_s)$, which is not directly transferred to the normal fluid. This loss of momentum is probably related to the generation and decay of the vortices. $\mathcal{I}F_s$ shows a resemblance to the pressure drops that can be calculated for viscous fluids. This remarkable result may possibly be explained by an intermediate role of the normal excitations. Larger vortices break down into smaller ones which may finally be reduced into rotons, meaning that the momentum flux or the pressure drop should depend on the normal viscosity. In turbulent flow a behaviour of the Blasius type may be reasonable. However, a Poiseuille-behaviour of the superfluid, as has been observed (see sections 2-3-3 and 4), is more difficult to understand.

An alternative way of describing the results for F_n and F_s may be in

terms of Reynolds numbers. For the normal fluid two Reynolds numbers may be of importance, defined with ρ_n and ρ respectively:

$$Re_v(n) = \frac{\rho_n v_n d}{\eta_n} \qquad \text{and} \qquad Re_v = \frac{\rho v_n d}{\eta_n} .$$

As was mentioned already, a laminar behaviour of the normal fluid was observed even in supercritical flow with $v_s \simeq 0$. Because of the limited level differences in the apparatus, the largest value of v_n that could be studied for turbulent flow in the wide capillary, was 16 cm/s at $T = 1.20$ K, corresponding with $Re_v(n) = 130$ and $Re_v = 3900$. In order to interpret their own results, Staas, Taconis and Van Alphen [14] did choose Re_v as the relevant Reynolds number and assumed the whole fluid to be turbulent at values of Re_v larger than the critical value 1200. The present results indicate that in our experiments Re_v seems to be irrelevant. Our results are not in contradiction with $Re_v(n)$ as the relevant Reynolds number. This is what should be expected if the two fluids behave separately in this aspect.

For the superfluid the experiments indicate that a relevant Reynolds number might be

$$Re_v(s) = \frac{\rho_s v_s d}{\eta_n} ,$$

since a 1.75th power dependence (Blasius) is found for F_s (e.g. at $v_n = 0$). In many cases the analogy with an ordinary viscous fluid is exact, i.e. the critical Reynolds number equals 1200. However, this is not always true: in some cases a different critical number has to be accepted in order to obtain a quantitative agreement. One may perhaps suppose that the critical Reynolds number depends on e.g. the normal fluid velocity. Further even with a critical Reynolds number of 1200, measuring points have been found on the ordinary unstable Blasius branch ($Re_v(s) < Re_v(s)_{cr}$, see flow with $v_n = 0$ and with $v_n = v_s$).

From the peculiar relation of F_{sn}/F_s on $(v_n - v_s)$ one might suppose that v_L, the velocity of the vortices, possibly deviates from v_s. Especially with $v_n > v_s$, a slip of the vortices relative to the superfluid might be present. At $v_n = v_s$, v_L equals v_s. It should be noted that with this type of flow ($v_n = v_s$), frictional forces (F_n and F_s) are still

acting on the normal fluid (F_n) and on the superfluid (F_s).

A possible entropy production in the flowing helium must be positive. Therefore one might suppose that an extra term in the equation of motion of the superfluid should contain a factor $(\vec{v}_n - \vec{v}_s)$ (see e.g. Lhuillier et al. [15]). Such a condition should probably be valid locally. In the present experiments only quantities integrated over the capillary can be obtained. Therefore the integrated force F_s need not be proportional to the mean relative velocity $(v_n - v_s)$. The only condition that has to be satisfied is that the entropy production must be positive. Since F_{sn}, F_n, and F_s change sign if respectively $(v_s - v_n)$, v_n, and v_s change sign, the condition of positive entropy production is indeed fulfilled.

A quantitative comparison of the results from Wiarda and Kramers on the second-sound attenuation with the results from the present study, is impossible so long the two-fluid model, with built-in vortices, is not further developed. The attenuation of second sound is closely connected with the total energy dissipation in turbulent flow. If two frictional forces are present (as e.g. F_s and F_{sn}), these two forces both supply positive contributions to the attenuation of second sound. A re-analysis of the results of Wiarda is still in progress.

References

1) Van der Heijden, G., De Voogt, W.J.P. and Kramers, H.C., to be published in Physica. (Commun. Kamerlingh Onnes Lab., Leiden, No.392a). The first chapter of this thesis.
2) Van der Heijden, G., Giezen, J.J. and Kramers, H.C., to be published in Physica. (Commun. Kamerlingh Onnes Lab., Leiden, No.394c). The second chapter of this thesis.
3) Gorter, C.J. and Mellink, J.H., Physica 15(1949)285 (Commun. Kamerlingh Onnes Lab., Leiden, Suppl. No.98a).
4) Van der Heijden, G., Van der Boog, A.G.M. and Kramers, H.C., Proc. of the 12th int. Conf. on low Temp. Phys., LT 12, Academic Press of Japan (Tokyo, 1971) p.65.
5) Atkins, K.R., Proc. Roy. Soc. A64(1951)833.
6) Kidder, J.N. and Fairbank, W.M., Proc. of the 7th int. Conf. on low Temp. Phys., LT 7, ed. Graham and Hollis Hallett, North-Holland Publ. Comp. (Amsterdam, 1961) p.560.
7) Kidder, J.N. and Fairbank, W.M., Phys. Rev. 127(1962)987.
8) Bhagat, S.M. and Mendelssohn, K., Cryogenics 2(1961)34.
9) Brewer, D.F. and Edwards, D.O., Phil. Mag. 6(1961)1173.
10) Bhagat, S.M. and Critchlow, P.R., Cryogenics 2(1961)39.
11) Hall, H.E. and Vinen, W.F., Proc. Roy. Soc. A238(1956)215.
12) Vinen, W.F., Proc. Roy. Soc. A242(1957)493.
13) Prandtl, L. and Tietjens, O.G., Applied Hydro- and Aeromechanics, Dover Publications (New York, 1934) p.37.
14) Staas, F.A., Taconis, K.W. and Van Alphen, W.M., Physica 27(1961)893 (Commun. Kamerlingh Onnes Lab., Leiden, No.328d).
15) Lhuillier, D., Vidal, F., Francois, M. and Le Ray, M., Phys. Letters to be published.

Samenvatting

In dit proefschrift worden metingen beschreven, die zijn verricht aan stromend vloeibaar helium beneden de lambda temperatuur. Verschillende typen stromingen door een nauw capillair zijn bestudeerd.

In hoofdstuk I wordt het stromingscircuit beschreven. De snelheden van de superfluïde en normale component van vloeibaar helium II kunnen onafhankelijk van elkaar, op van te voren vast te stellen waarden, ingesteld worden. Zowel stromingen waarbij de twee fluïda dezelfde kant op stromen als waarbij ze tegen elkaar in stromen zijn onderzocht. Uit het gemeten temperatuurverschil over het capillair en uit een gemeten hoogteverschil kunnen de fonteindruk ($\rho S \Delta T$), het chemisch potentiaal verschil ($\rho \Delta \mu$) en het drukverschil (ΔP) over het capillair bepaald worden. De resultaten van meetseries waarin de gemiddelde superfluïde snelheid (v_s) ongeveer nul is, worden in hoofdstuk I beschreven. In hoofdstuk II worden de resultaten van stromingen waarin de gemiddelde snelheid van het normale fluïdum (v_n) ongeveer nul is gegeven, terwijl in hoofdstuk III meetseries waarin v_s en v_n beide ongelijk aan nul zijn, behandeld worden. Er werden twee typen stromingen waargenomen: subcritische stromingen zonder chemisch potentiaal verschil over het capillair ($\rho \Delta \mu \equiv 0$), die dus voldoen aan de London relatie, en supercritische (turbulente) stromingen waarin $\rho \Delta \mu \neq 0$.

De verkregen meetresultaten worden beschreven met behulp van drie krachten: F_n, F_{sn} en F_s. De kracht F_n, de visceuze wrijvingskracht, die op het normale fluïdum werkt, blijkt zowel in sub- als in supercritische stromingen een laminair gedrag van het normale fluïdum te beschrijven. De wederkerige wrijvingskracht F_{sn} beschrijft de wisselwerking van de twee fluïda in turbulente stromingen. De wrijvingskracht F_s, die alleen op het superfluïdum werkt, blijkt een zekere verwantschap te vertonen met de wrijvingskracht, die optreedt in gewone visceuze vloeistoffen.

De resultaten zijn weergegeven in diagrammen in het (v_n, v_s) vlak met lijnen van constante $\rho S \Delta T$, $\rho \Delta \mu$ en ΔP (fig. 10, 11 en 12). Uit deze diagrammen kan afgeleid worden bij welke snelheidscombinaties (v_n, v_s) een isotherme stroming ($\Delta T = 0$) optreedt. In een bepaald gebied van het (v_n, v_s) vlak konden geen stationaire stromingen geproduceerd worden, omdat de ingestelde grootheden bleven oscilleren.

De totale gevonden druk blijkt de som te zijn van een Poiseuille bijdrage van het laminair stromende normale fluïdum en een bijdrage van het turbulente superfluïdum. Ook isobare stromingen ($\Delta P = 0$) zijn mogelijk, wanneer het superfluïdum en het normale fluïdum tegen elkaar in stromen en de twee bijdragen tot de totale druk ΔP elkaar compenseren.
Uit de waarnemingen kan afgeleid worden dat het normale fluïdum ook laminair stroomt, als het superfluïdum turbulent is. In deze experimenten blijkt turbulentie dus alleen maar een eigenschap van het superfluïdum te zijn.

Er blijkt een universeel verband te zijn tussen de verhouding F_{sn}/F_s en de relatieve snelheid $(v_n - v_s)$, hetgeen suggereert dat zowel F_{sn} als F_s afhangen van de gemiddelde lengte aan wervellijnen per eenheid van volume. Getracht is een verklaring te vinden voor de relatie van F_{sn}/F_s en $(v_n - v_s)$, door aan te nemen dat de wervellijnen onder invloed van het normale fluïdum ten opzichte van het superfluïdum kunnen bewegen.

Teneinde te voldoen aan het verzoek van de faculteit der Wiskunde en Natuurwetenschappen, volgt hier een kort overzicht van mijn studie.

Nadat ik in 1956 het diploma HBS-B had behaald aan het Christelijk Lyceum te Alphen aan de Rijn, begon ik in september 1956 mijn studie aan de Rijksuniversiteit te Leiden. Het candidaatsexamen in de wis- en natuurkunde met bijvak sterrekunde (A) legde ik af in 1961, het doctoraal examen experimentele natuurkunde in 1964.

Sinds november 1961 ben ik op het Kamerlingh Onnes Laboratorium werkzaam in de werkgroep Helium II, die onder leiding staat van Dr. H.C. Kramers. Aanvankelijk assisteerde ik Drs. P.L.J. Cornelissen bij zijn metingen aan de warmtegeleiding van vloeibaar helium, daarna werkte ik bij Dr. T.M. Wiarda aan een onderzoek naar de demping van het tweede geluid. In 1965 begon ik met het onderzoeken van stromingsverschijnselen in He II. In oktober 1967 werd een begin gemaakt met de in dit proefschrift beschreven experimenten.

Sinds 1963 heb ik tevens geassisteerd op het natuurkundig practicum en vanaf 1968 was ik belast met de leiding van het werkcollege behorende bij het college Elementaire Statistische Fysica van Dr. H.C. Kramers.

Velen hebben bijgedragen aan het welslagen van het onderzoek in dit proefschrift vermeld.

Bij het uitvoeren van de experimenten heb ik achtereenvolgens samengewerkt met Drs. R.J. Kolderman, Drs. J.J. Giezen, Drs. W.J.P. de Voogt, Drs. A.G.M. van der Boog, P.J.J. Peters en R.R. IJsselstein.
De constructie van de gebruikte apparaten en de cryogene voorzieningen werden verzorgd door de heren T. Nieboer en J. van den Berg, terwijl de heer J.W. Groenewold verscheidene onderdelen vervaardigde. De tekeningen van dit proefschrift werden gemaakt door de heren H.J. Rijskamp en W.F. Tegelaar, terwijl laatstgenoemde ook de foto's verzorgde.

Dr. R.C. Thiel en Dr. H. van Beelen ben ik dank verschuldigd voor hun kritische opmerkingen en de correctie van de Engelse tekst.

Mevr. A.W. van der Heijden-Swaneveld heeft het typewerk voor dit proefschrift verzorgd.